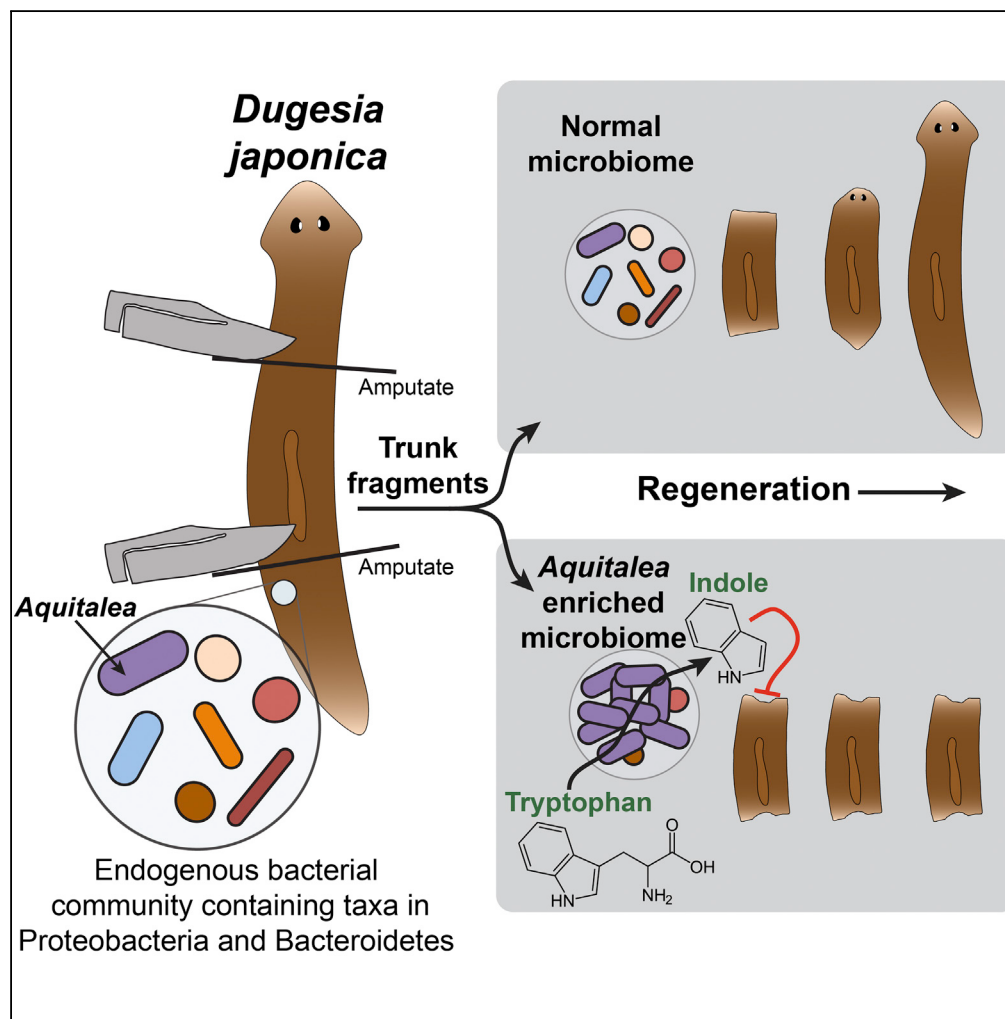


Article

The Bacterial Metabolite Indole Inhibits Regeneration of the Planarian Flatworm *Dugesia japonica*



Fredrick J. Lee,
Katherine B.
Williams, Michael
Levin, Benjamin E.
Wolfe

frederick.lee@tufts.edu (F.J.L.)
benjamin.wolfe@tufts.edu
(B.E.W.)

HIGHLIGHTS

The planarian worm *Dugesia japonica* is colonized by Bacteroidetes and Proteobacteria

Many of these bacteria can be cultured and experimentally manipulated

Some bacteria can inhibit regeneration, including eye and blastema formation

Indole produced by planarian-associated bacteria contributes to regeneration delays

Lee et al., iScience 10, 135–148
December 21, 2018 © 2018
The Author(s).
<https://doi.org/10.1016/j.isci.2018.11.021>



Article

The Bacterial Metabolite Indole Inhibits Regeneration of the Planarian Flatworm *Dugesia japonica*

Fredrick J. Lee,^{1,3,*} Katherine B. Williams,^{1,3} Michael Levin,^{1,2} and Benjamin E. Wolfe^{1,4,*}

SUMMARY

Planarian flatworms have been used for over a century as models for regeneration. Planarians live in aquatic environments with constant exposure to microbes, but the mechanisms by which bacteria may mediate planarian regeneration are largely unknown. We characterized the microbiome of laboratory populations of the planarian *Dugesia japonica* and determined how individual bacteria impact *D. japonica* regeneration. Eight to ten taxa in the phyla Bacteroidetes and Proteobacteria consistently occur across planarian colonies housed in different research laboratories. Individual members of the *D. japonica* microbiome can delay regeneration including the development of eye spots and blastema formation. The microbial metabolite indole is produced in significant quantities by two bacteria that are consistently found in the *D. japonica* microbiome and contributes to delays in regeneration. Collectively, these results provide a baseline understanding of the bacteria associated with the planarian *D. japonica* and demonstrate how metabolite production by host-associated microbes can affect regeneration.

INTRODUCTION

The past decade of host microbiome research has rapidly revealed the diversity of microbial communities that live in and on eukaryotic hosts and their potential roles in mediating host biology (McFall-Ngai et al., 2013). Much of this research has focused on contributions of microbes to host metabolism, physiology, and immunology. In a variety of animals, microbial communities have been shown to aid in the provision of nutrients (Sannino et al., 2018; Wong et al., 2014), alter immune system function (Brestoff and Artis, 2013; Lee and Mazmanian, 2010), and shape host behavior (Sampson and Mazmanian, 2015; Vuong et al., 2017).

One aspect of host biology wherein contributions of the microbiome are poorly characterized is regeneration. Regeneration, which is defined as the ability to replace and repair body parts that are severely damaged (e.g., amputation), is a unique feature of certain metazoans (Sánchez Alvarado, 2000; Sánchez Alvarado and Tsonis, 2006). The ability to regenerate tissues or organs spans the kingdom Animalia, with certain species able to completely regenerate entire organ systems and body parts (i.e., planarian worms and *Hydra*), others possessing the capability to replace entire limbs or organs (i.e., zebrafish and axolotls), and others with limited regenerative abilities (i.e., humans and mice) (Bely and Nyberg, 2010; Brockes and Kumar, 2008; Holstein et al., 2003; Sánchez Alvarado, 2000; Sánchez Alvarado and Tsonis, 2006). Regeneration in multicellular organisms requires the detection of trauma, activation of repair processes, production and differentiation of new cells, and coordinated arrangement of tissues into organ systems (Brockes and Kumar, 2005; Tanaka and Reddien, 2011). All these events require a complex interplay of multiple biophysical and biochemical processes, each of which could potentially interface with bacteria-derived signals.

Host-associated microbes could potentially mediate the outcomes of regeneration through several different processes. First, pathogenic microbes could infect regenerating wound sites and directly inhibit regenerating tissues by killing host cells. Previous work on the microbiology of wounds has documented how microbes can influence wound-healing outcomes (Edwards and Harding, 2004; Eming et al., 2014), but studies on how microbes can impact whole organ or limb regeneration are limited. Second, non-pathogenic microbes could promote or inhibit regeneration by secreting metabolites at wound sites that alter the cellular processes necessary for normal patterning in host tissues. Finally, microbes could promote and accelerate regeneration by inhibiting the growth of microbial species that inhibit regeneration, by secreting metabolites that promote host regeneration, or by inducing host cellular processes that promote

¹Allen Discovery Center at Tufts University, Medford, MA 02155, USA

²Wyss Institute for Biologically Inspired Engineering, Harvard University, Boston, MA 02115, USA

³These authors contributed equally

⁴Lead Contact

*Correspondence:
frederick.lee@tufts.edu
(F.J.L.),
benjamin.wolfe@tufts.edu
(B.E.W.)

<https://doi.org/10.1016/j.isci.2018.11.021>



tissue repair. Numerous studies have demonstrated that microbes can secrete metabolites that affect host biology (Koppel and Balskus, 2016; Postler and Ghosh, 2017; Sharon et al., 2014), but we are unaware of studies that have considered how microbial metabolites can influence regeneration processes.

Over the past century, planarian flatworms have been used as model organisms to understand mechanisms of metazoan regeneration. Planarian worms harbor specific populations of fully pluripotent cells (neoblasts) that, upon trauma, become highly active and proliferate at the site of injury to form a cluster of new undifferentiated cells called a blastema (Durant et al., 2016; Lobo et al., 2012; Reddien and Sánchez Alvarado, 2004). The blastema cells then differentiate and serve as the basic cellular units for building and replacing tissues, organs, and body parts. The entire process of regeneration is temporally regulated by the expression of a variety of host genes (Durant et al., 2016; Lobo et al., 2012; Reddien and Sánchez Alvarado, 2004). Planarian worms are capable of regenerating entire individuals from small body fragments (Morgan, 1898). These worms live in natural and laboratory aquatic ecosystems wherein wound sites are exposed to microbes.

Despite the importance of planarians as models for regeneration, the microbiome of planarians and impacts of microbes on planarian regeneration are poorly characterized. A recent study characterized the microbiome of one planarian species (*Schmidtea mediterranea*) and demonstrated that one bacterial member of the *S. mediterranea* microbiome, a *Pseudomonas* species, can elicit a pathogenic response in the host that inhibits regeneration (Arnold et al., 2016). These findings provided the first evidence that microbes can mediate planarian regeneration, but they did not identify mechanisms by which bacteria alter the regenerative process in planarians. Furthermore, it is also unclear whether the previously described microbiome diversity is conserved across other planarian species.

In this study, we describe the diversity of the microbes associated with laboratory populations of the planarian worm *Dugesia japonica* and demonstrate that individual bacteria within the *D. japonica* microbiome can mediate regeneration outcomes. *D. japonica* is a close relative to *S. mediterranea* and is widely used in studies of regeneration (Álvarez-Presas et al., 2008; Gentile et al., 2011), yet very little is known about its microbiome (Morokuma et al., 2017). By using 16S rRNA sequencing of DNA and RNA, culture-based approaches, and whole-genome sequencing, we characterized the diversity of the *D. japonica* microbiome across time and across multiple laboratories. By manipulating the *D. japonica* microbiome through inoculation experiments, we also assessed the roles of individual bacterial species in mediating regeneration outcomes. We identified one common microbiome member, a non-pathogenic Aquitalea species (class Betaproteobacteria), that substantially delays regeneration after tail and head amputation. Production of the metabolite indole by Aquitalea can also delay regeneration, providing a mechanistic link between the planarian microbiome and the regeneration processes.

RESULTS

D. japonica Worms Have a Consistent Bacterial Community

To determine the bacterial composition of laboratory-reared *D. japonica*, we used high-throughput amplicon sequencing of the 16S rRNA gene. We obtained an initial profile of the bacterial diversity of our worms by sampling individual worms at three times over the course of a year (2016–2017). On average, a single worm harbors 42 distinct bacterial operational taxonomic units (OTUs) using a threshold of 97% sequence similarity. Across all worms, eight OTUs accounted for approximately 80% of the bacterial community, with Bacteroidetes and Proteobacteria dominating the communities (Figure 1A, Table S1). On average, Bacteriodetes taxa (i.e., *Taibaiella* sp. OTU003 and *Pedobacter* sp. OTU001) accounted for 36% of the sequence data, while Proteobacteria (i.e., *Paucibacter* sp. OTU011, *Rhodoferax* sp. OTU019, *Comamonadaceae* sp. OTU002, *Burkholderiales* sp. OTU005, and *Aquitalea* sp. OTU004) accounted for 40%. Across the three sampling times, these taxa were consistently present, but their relative abundance varied across individuals (Figure 1A).

In an effort to culture bacterial strains representative of taxa observed in our 16S rRNA survey, worm homogenates were plated on several types of media and conditions (see Methods), and unique bacterial strains were isolated based on colony morphology (Figure 1B). Four isolates were in the phyla Bacteroidetes (*Chryseobacterium* sp. KBW03, *Pedobacter* sp. KBW01PK, and *Pedobacter* sp. KBW06S, and *Taibaiella* sp. KBW10), five were β-Proteobacteria species (*Variovorax* sp. KBW07, *Acidovorax* sp. FJL06, *Oxalobacteraceae* sp. KBW02, *Paucibacter* sp. KBW04, and *Aquitalea* sp. FJL05), and one was a

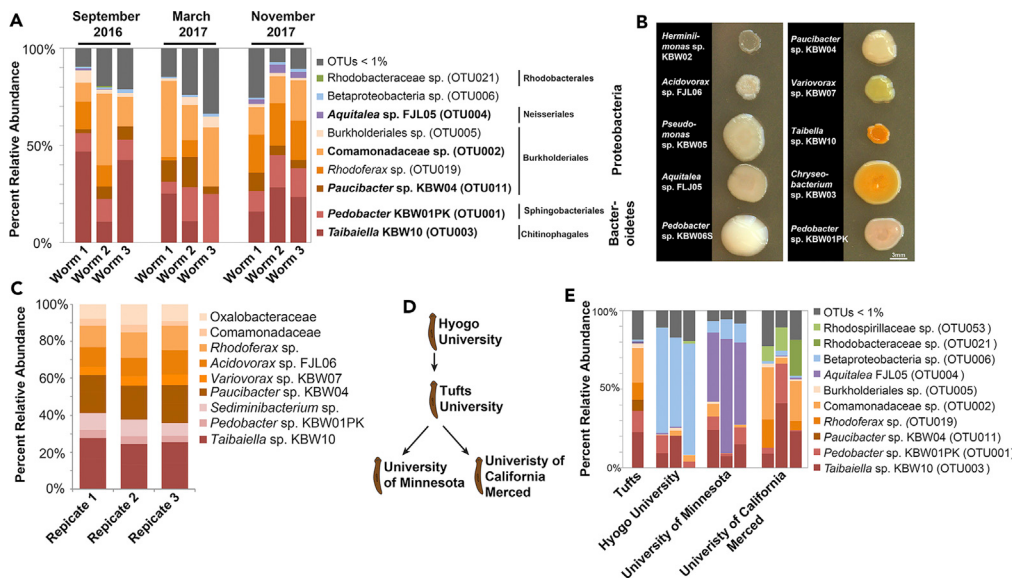


Figure 1. Microbiome Diversity of the Planarian *Dugesia japonica*

(A) Bacterial community composition of three individual worms was determined at three time points using 16S rRNA gene amplicon sequencing. OTUs >1% relative abundance are shown. See [Table S1](#) for full list of OTUs. OTUs highlighted in bold have cultured representatives.

(B) Spots of bacterial cultures on brain heart infusion agar from some of the most abundant and culturable bacteria in the *D. japonica* microbiome.

(C) 16S rRNA transcript mining of the *D. japonica* microbiome. Total RNA extracted from pooled sets of worms were synthesized into cDNA libraries and sequenced with the Illumina HiSeq platform, and the reads were mapped to a custom 16S rRNA database (see [Methods](#)). Reference sequences with $\geq 1.5\%$ of mapped reads are shown. Each column represents a biological replicate of five worms. See [Table S4](#) for the full list of reference sequences.

(D) History of the *D. japonica* strain GI across four laboratories.

(E) *D. japonica* microbiome diversity across four laboratories. The first column on the left is the average of Tufts data from (A). Each column represents a single worm.

See also [Figures S1](#) and [S2](#) and [Tables S1](#), [S2](#), [S3](#), [S4](#), and [S5](#).

γ -Proteobacteria (*Pseudomonas* sp. KBW05) ([Figure S1](#)). Collectively, we were able to culture bacterial strains that represent five of the seven OTUs that make up over 75% of the diversity in our 16S rRNA survey ([Table S1](#)). To confirm the identity of isolates and acquire additional information on functional potential, draft genomes were assembled and annotated for each of these dominant bacterial taxa ([Table S2](#)).

To identify potentially active bacteria associated with *D. japonica*, we extracted total RNA from three pools of five worms and sequenced cDNA libraries ([Tables S3](#) and [S4](#)). Across the three libraries, 11 taxa dominated transcription in the worm microbiome, with Bacteroidetes and β -Proteobacteria accounting for 36% and 64%, respectively, of 16S rRNA transcripts for taxa above a 1.5% relative abundance threshold. Many of the bacteria identified in our 16S rRNA amplicon sequencing and culturing efforts were also identified as active in the worm microbiome ([Figure 1C](#)). For example, of the three Bacteroidetes species identified in our analysis, *Taibaiella* sp. was the most transcriptionally active. These results are recapitulated in our 16S rRNA survey wherein *Taibaiella* is typically observed as a highly abundant species across worm samples.

D. japonica planaria are used across many laboratories as models for regeneration. To determine if the bacterial communities associated with *D. japonica* are consistent across different laboratory populations, we sampled the microbiome of the same clonal population of *D. japonica* shared across three additional laboratories. The *D. japonica* worms in our laboratory at Tufts originated from the Umesono laboratory in Japan (Hyogo University) and were later used to seed and start colonies in subsequent laboratories (Marchant lab at the University of Minnesota; Oviedo lab at the University of California, Merced; [Figure 1D](#)). These worms are all of the same genetic background and are known as the “GI strain” or sometimes “Dj-GI.” Worm care practices differ between laboratories ([Table S5](#)), and we predicted that this might impact the

microbiome composition of *D. japonica* across the different worm colonies. A total of 10 OTUs from the phylum Bacteroidetes and Proteobacteria dominated the *D. japonica* microbiome across laboratories (Figure 1E). Nine of these OTUs were also the dominant taxa in our Tufts University worm colony. Across the four laboratories, some taxa ranged widely in relative abundance (Figure S2; Table S1). For example, *Aquitalea* sp. OTU004, was observed across all laboratory-reared worms, with a high abundance of *Aquitalaea* sp. (56% relative abundance) in the University of Minnesota worms and a low abundance in other laboratories (<1%–10% relative abundance).

Spatial Variation and Stability of the *Dugesia japonica* Microbiome

To better understand what factors shape the diversity of the *D. japonica* microbiome, we assessed the spatial structure and stability of bacterial communities associated with *D. japonica*. For all of this work, we used a culture-based method to determine bacterial community composition because we found that much of the *D. japonica* microbiome can be cultured and because we are ultimately interested in the dynamics of bacteria that can be easily manipulated in regeneration experiments. We acknowledge that some rare or difficult-to-culture taxa that were observed in 16S rRNA sequencing efforts may be missed with this approach.

Many planarian regeneration experiments use head, trunk, and tail fragments in regeneration assays (Lander and Petersen, 2016; Lobo and Levin, 2015; Petersen and Reddien, 2008; Reddien and Sánchez Alvarado, 2004). To determine whether these various body fragments are colonized by distinct bacterial communities, we divided individual worms ($n = 6$) into these three fragments (Figure 2A) and plated worm homogenates onto brain heart infusion agar to determine the bacterial community composition. The composition of bacterial communities across the head, trunk, and tail fragments was highly variable across individual worms (Figure 2A), but we did not detect statistically significant differences in bacterial community composition across these three regions (PERMANOVA, $F = 2.16$, $p = 0.08$). None of the bacterial taxa were significantly enriched in any of the body fragments. This suggests limited spatial structure at the coarse scale of whole worm bodies and a well-mixed bacterial community across *D. japonica*.

Planarian worms have distinct external and internal features that may create unique environments for specific bacterial communities. For example, worms have a distinct gastrovascular tract inside their bodies and secrete significant quantities of mucus on their external surfaces (Hayes, 2017; Pedersen, 1963). To better understand whether bacterial taxa are unevenly distributed across external and internal components of the worm, we used a fractionation approach. Externally associated bacteria were detected after gently washing worms in 1X phosphate buffered saline, and internally associated bacteria were detected in the remaining worm homogenate after washing (see Methods for details). The gastrovascular tract cannot be easily dissected from planarian worms, so we were unable to specifically assess the gut microbiome of the worms. The relative abundance of *Chryseobacterium* sp. was higher in the external fraction than in the internal fraction (external = $65.7\% \pm 17\%$ relative abundance, internal = $24.7\% \pm 19\%$ relative abundance) (Figure 2B). Two other bacteria, *Polaromonas* sp. and *Pedobacter* sp. KBW01PK, were not detected in the external fraction and were exclusively found in the internal fraction. No significant differences between the external and internal fractions were observed for the other major bacterial taxa isolated from these worms (*Pseudomonas* sp., *Herminiimonas* sp., *Variovorax* sp., *Pedobacter* sp. KBW06S, and *Taibaiella* sp.).

Our survey of *D. japonica* across laboratories from a common origin demonstrated that some bacterial taxa were unique to specific worm colonies. This suggests the potential for *D. japonica* worms to pick up and/or lose bacterial species in response to changing environments. To experimentally assess plasticity of the *D. japonica* microbiome, we tested whether exogenous microbes that are not normally associated with *D. japonica* can establish within the *D. japonica* microbial community. We placed worms in an inoculum of exogenous microbes that were previously isolated from various aquatic systems, including a laboratory population of axolotls (*Ambystoma mexicanum*), a laboratory population of the South African clawed frog (*Xenopus laevis*), and a freshwater pond in a garden in Boston. We also tested a common laboratory strain of *E. coli*. After removing the worms from this inoculum and placing them in sterile water, we destructively sampled worms at different time points over the course of 15 days (Figure 2C).

Some exogenous microbes were detected at 1 and 4 days after being removed from the inoculum, whereas at 15 days we no longer detected any of the exogenous microbes (Figure 2C). These results indicate that *D. japonica* does not readily associate with environmental bacteria and that exogenous microbes may have difficulty colonizing an established microbiome of *D. japonica*. This observation is consistent with previous

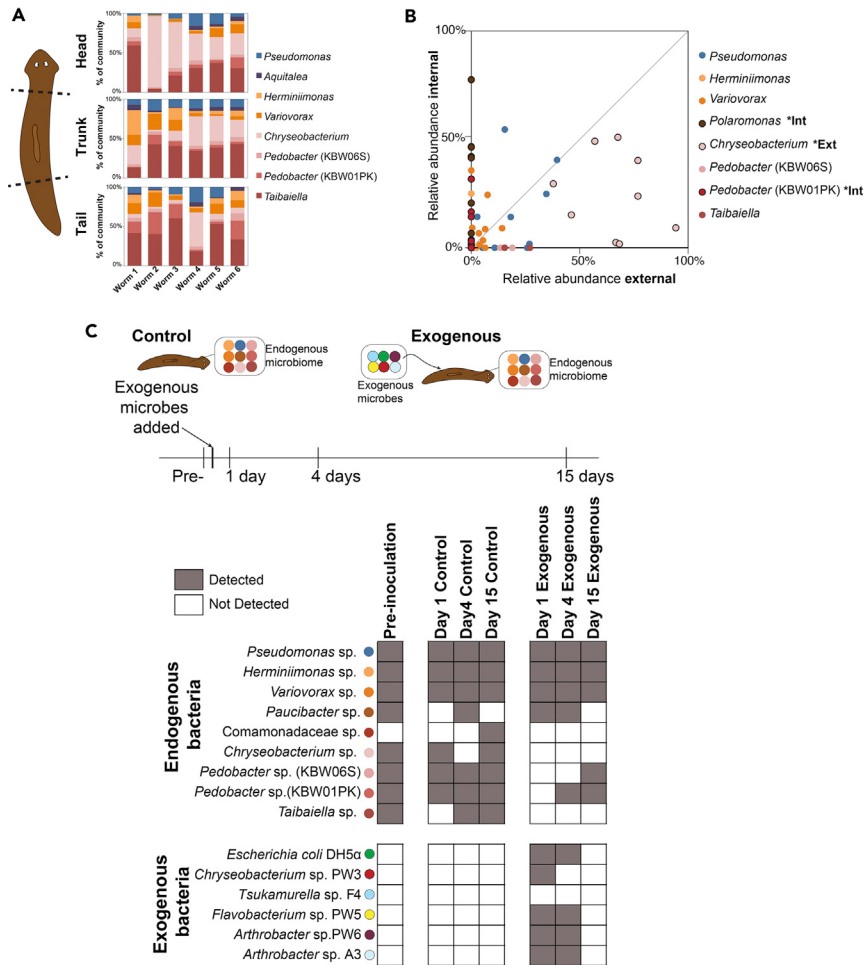


Figure 2. Spatial Variation and Stability of the *Dugesia japonica* Microbiome

(A) Bacterial community composition across the head, trunk, and tail fragments of individual worms. Data show relative abundance of culture-based (plating on brain heart infusion agar) bacterial community composition.

(B) Relative abundance of *D. japonica*-associated bacteria on the external surfaces and within internal components of individual worms. Each point represents the relative abundance for each worm sampled. *Int, bacterium enriched in internal fraction; *Ext, bacterium enriched in external fraction.

(C) Experimental assessment of the ability of exogenous microbes to colonize the *D. japonica* microbiome. Detected, taxa detected at >1% of the total bacterial community using culture-based approach (plating on brain heart infusion agar); not detected, <1% the total bacterial community.

reports that *D. japonica* is not readily colonized after exposure to pathogenic bacteria (Abnave et al., 2014). Some endogenous microbes, including *Chryseobacterium* and *Taibaiella*, were not detected in worms wherein exogenous microbes were added. They may have been present in very low abundances but were below the detection limit of our culture-based method or may have been displaced by the addition of exogenous microbes. This work did not specifically address how exogenous microbes may affect the endogenous bacterial community of *D. japonica*, but the role of microbe-microbe interactions in shaping the *D. japonica* microbiome is a promising area of future investigation. We also acknowledge that these experiments have only tested just a few easy-to-isolate bacteria. The unique bacterial species detected in *D. japonica* microbiomes from different laboratory populations may be present due to rare invasion events of bacterial taxa not examined here.

Bacteria Associated with *D. japonica* can Delay Regeneration

Our results described above provide a baseline understanding of the microbes that inhabit this planarian species and their dynamics over space and time in laboratory cultures. To determine whether any of the

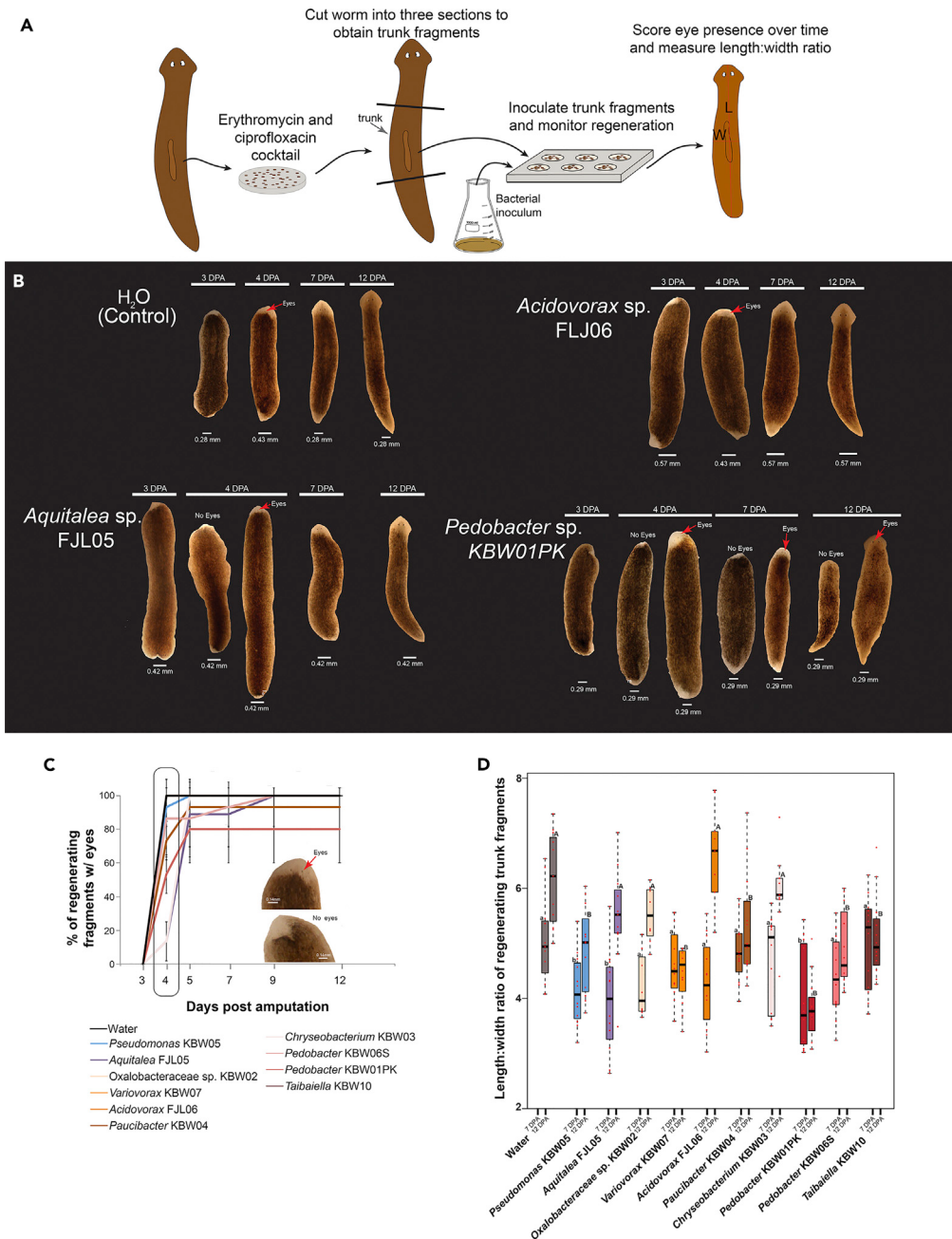


Figure 3. A Regeneration Screen of the *Dugesia japonica* Microbiome Demonstrates Bacterial-Induced Delays in Regeneration

- (A) Overview of the experimental design of the regeneration screen.
- (B) Representative images of the regenerative progress of trunk fragments treated in bacterial inocula or sterile worm water over the course of 12 days. Worm images were cropped to remove background shadows using the Magic Eraser Tool in Adobe Photoshop. Uncropped images from other bacterial treatments can be found in [Figure S4](#).
- (C) Frequency of trunk fragments with eye spots in different bacterial treatments. Many treatments reached 100% at day 4, so they are not visible (are under the Water line). Inset shows examples of worms with and without eyes 4 days post-amputation. Error bars represent \pm standard deviation.
- (D) Length-to-width ratios of worms at 7 and 12 days post-amputation (DPA). Red dots represent data for individual worms, and boxplot shows mean and standard deviation. Welch's t test determined statistical difference in

Figure 3. Continued

length-to-width ratios when comparing water controls and bacterial treatments at 7 DPA ($F_{(10, 45)} = 2.68, p = .011$) and 12 DPA ($F_{(10, 42)} = 12.0, p < 0.001$). Bonferroni corrected post-hoc analysis identified bacterial treatments statistically different from the respective water control at 7 DPA (lowercase letters indicate statistical differences; $p < 0.005$) and 12 DPA (uppercase letters indicate statistical differences; $p < 0.001$). Error bars represent \pm standard deviation.

See also Figures S3 and S4 and Table S6.

identified bacteria impact *D. japonica* regeneration, we conducted a regeneration screen wherein the head and tail of fully regenerated worms were aseptically amputated and the remaining trunk fragment submerged into pure cultures of bacteria (Figure 3A). We were unable to generate completely germ-free planarian worms due to difficulties in maintaining worms in antibiotics for long periods of time (Miller et al., 1955). We instead used a short-term antibiotic treatment and bacterial inoculation approach to manipulate the *D. japonica* microbiome. Before the screen, fully regenerated worms were subjected to an antibiotic cocktail, which significantly depletes the bacterial load without affecting host regeneration (Figure S3). The bacterial densities used in our screen (Table S6) are similar to what were used in a previous study of regeneration in a different planarian species (Arnold et al., 2016). Over the course of two weeks, regenerative progress was monitored and compared to that of fragments regenerating in sterile water.

Bacterial treatments displayed a broad range of effects on host regeneration (Figure 3B). For example, *Acidovorax* sp. FJL06, *Oxalobacteraceae* sp. KBW02, *Taibaiella* sp. KBW10, and *Variovorax* sp. KBW07 had no major effect on *D. japonica* regeneration (Figure 3B). All other bacterial inocula caused delays in host eye development. For example, certain bacterial treatments (*Aquitalea* sp. FJL05, *Chryseobacterium* sp. KBW03, *Pedobacter* sp. KBW06S, and *Pseudomonas* sp. KBW05) caused a delay in eye development for a proportion of individuals in a population, with all regenerating fragments acquiring eyes 9 days post-amputation (Figure 3B). A similar observation was made for *Pedobacter* sp. KBW01PK and *Paucibacter* sp. KBW04, except that a subset of individuals subjected to these bacterial inocula remained without eye spots at the conclusion of the study (Figure 3B).

To better understand how bacterial treatments impacted eye spot development, we quantified the presence of eye spots on the anterior end (i.e., head) of regenerating fragments from the regeneration screen described above. Up to three days post-amputation, eye spots were not visible for any treatment condition, including the water control (Figures 3B, 3C, and S4). By 5 days post-amputation, eye spots were observed for all or at least a proportion of regenerating fragments in all treatment conditions (Figure 3C). The most striking difference in eye development was observed at 4 days post-amputation, wherein the average number of worm fragments with eyes was significantly lower, compared with the control treatment, for the following inocula: *Aquitalea* sp. FJL05, *Pedobacter* sp. KBW01PK, *Chryseobacterium* sp. KBW03, and *Paucibacter* sp. KBW04 (Kruskal-Wallis test with Mann-Whitney U post-hoc tests, $p < 0.001$).

In addition to quantifying eye development trends, we also tracked the overall shape of the regenerating fragments at 7 and 12 days post-amputation. During typical regeneration of trunk fragments, sites of amputated tissue contract, initiating healing and remodeling processes (Beane et al., 2013; Oviedo et al., 2003; Reddien and Sánchez Alvarado, 2004; Tettamanti et al., 2008). Over the course of a few days, a cluster of self-renewing cells form a blastema, which governs the process of regenerating new tissues that will eventually become a new head and tail, on the respective anterior and posterior end of the trunk fragment (Aboobaker, 2011; Agata and Watanabe, 1999). By 7 days post-amputation, fragments have constructed a new head and tail that continue to develop, while the entire planarian body undergoes remodeling of tissues throughout the entire organism, with the ultimate goal of acquiring morphological body plan that is identical to a fully regenerated worm (Beane et al., 2013). Fragments in early stages of regeneration are shorter in body length and wider in body width, whereas fully regenerated worms have a target morphology that is longer and slimmer. Therefore, body length-to-width ratio is a useful metric to track the normal process of tissue remodeling in planarians (Emmons-Bell et al., 2015; Scimone et al., 2017).

Our initial analysis of body dimensions focused on comparing the length-to-width ratio of control and bacteria-treated worm fragments at 7 days post-amputation. This time point was selected because it is the earliest time point at which nearly all regenerating fragments in our study had eyes and regenerated head and tail structures. *Aquitalea* sp. FJL05, *Pseudomonas* sp. KBW05, and *Pedobacter* sp. KBW01PK

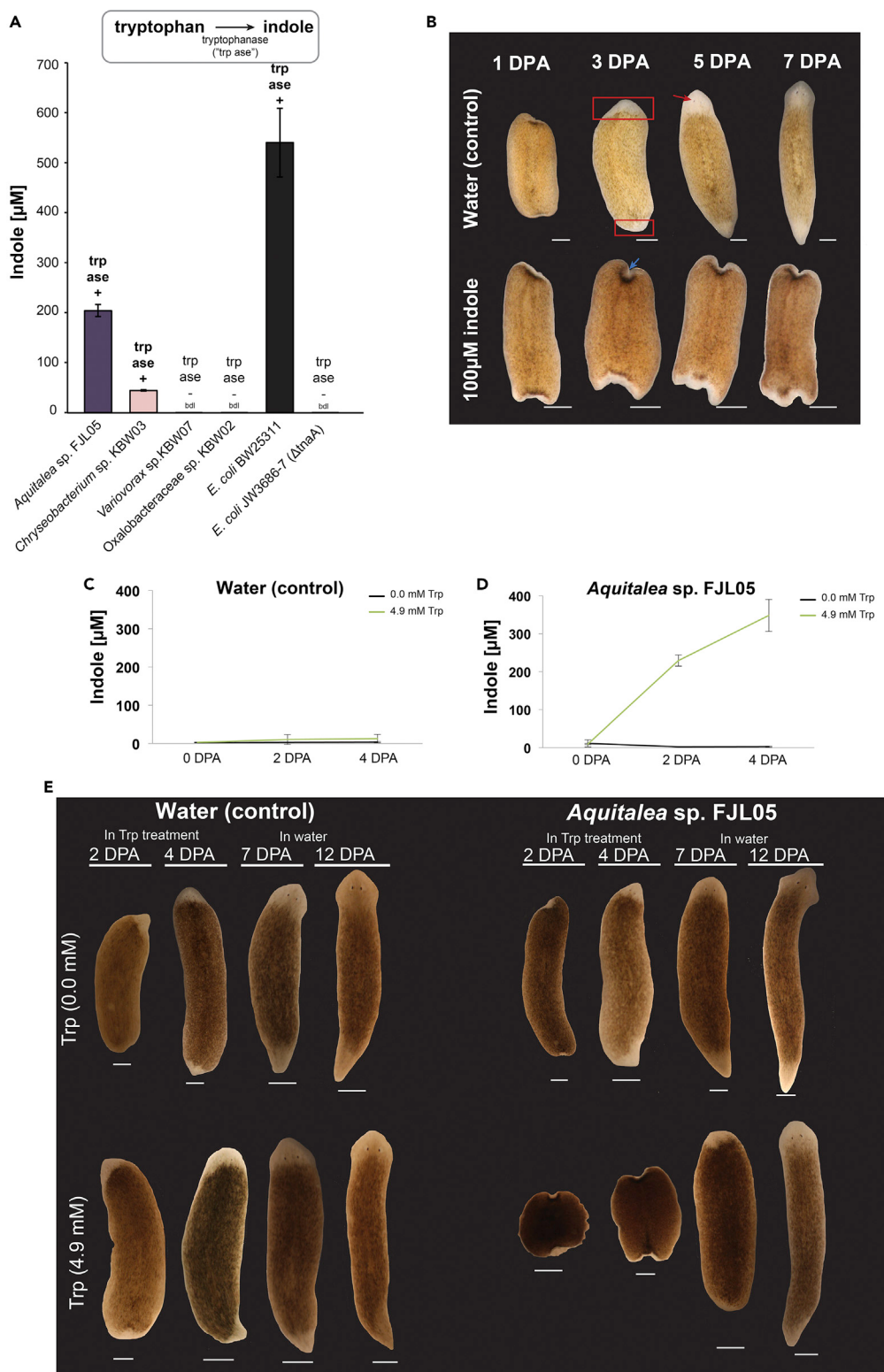


Figure 4. Indole as a Mechanism Underlying Bacterial Delays in Regeneration

(A) Production of indole in tryptophan broth by bacteria isolated from the *Dugesia japonica* microbiome and by control (BW25311) and *tnaA* mutant (JW3686-7) *E. coli* strains. Indole was quantified colorimetrically using the HIA assay. Bars

Figure 4. Continued

represent means and error bars represent \pm standard deviation; trp ase+ means the *tnaA* gene was detected in the genome of the indicated bacterium; bdl, below detection limit of HIA assay.

(B) Impacts of pure indole on *D. japonica* regeneration from 1–7 days post-amputation (DPA). White scale bar for each worm, 0.44 mm. Red rectangles indicate formation of a blastema at the anterior and posterior ends of the regenerating trunk fragment. Red arrow indicates eye spots. Blue arrow indicates lack of blastema formation.

(C and D) Indole production in (C) water control and in (D) *Aquitalea* inoculum with and without supplemental tryptophan. Lines represent means and error bars represent \pm standard deviation.

(E) Regeneration phenotypes observed in water control and *Aquitalea* inoculum with and without supplemental tryptophan. Data for Oxalobacteraceae sp. KBW02 and *E. coli* strains can be found in Figure S6. White scale bar for each worm, 0.44 mm.

See also Figure S5.

inocula significantly altered the length-to-width ratio, producing regenerating worm fragments with a lower ratio (i.e., worm fragments possessed a shorter and wider morphology), indicating slower remodeling of host tissues (Figure 3D). This is consistent with the observed delay in eye development for worm fragments treated in *Aquitalea* sp. FJL05 and *Pedobacter* sp. KBW01PK inocula (Figure 3C). Conversely, no statistically significant effect on host length-to-width ratio was observed for *Chryseobacterium* sp. KBW03 or *Paucibacter* sp. KBW04 treatments, even though we observed delays in eye development (Figure 3C).

Analysis of length-to-width ratios at 12 days post-amputation revealed shifts from the 7 days post-amputation dataset with *Pedobacter* sp. KBW01PK, *Pedobacter* sp. KBW06S, *Pseudomonas* sp. KBW05, *Taibaiella* sp. KBW10, and *Variovorax* sp. KBW07 displaying statistically lower ratios than worm fragments that regenerated in water (Figure 3D). Out of the five bacterial inocula identified to negatively impact the length-to-width ratio of regenerating fragments at 12 days post-amputation, *Pedobacter* sp. KBW01PK and *Pseudomonas* sp. KBW05 were observed to cause delays in eye development and/or remodeling of worms 7 days post-amputation (Figures 3B, 3C, and S4). Conversely, *Pedobacter* sp. KBW06S, *Taibaiella* sp. KBW10, and *Variovorax* sp. KBW07 were only observed to delay remodeling of regenerating worms at 12 days post-amputation. Although the reported delays in host regeneration could be partially due to bacterial infection, there were no direct indications that worms harbored a systemic infection. In all treatment conditions, regenerating fragments appeared healthy with no observed lesions in tissues, a common sign of infection (Arnold et al., 2016).

Indole Production by *Aquitalea* Delays Regeneration of *D. japonica*

Our results mentioned above demonstrate that bacterial taxa in the *D. japonica* microbiome can delay regeneration. We next sought to identify potential molecular mechanisms underlying this bacterial control of host regeneration. During our efforts to culture microbes from the *D. japonica* microbiome, we noticed that certain bacterial inocula exuded strong fecal and barnyard odors that were reminiscent of indole-producing bacteria from other microbial systems studied in our laboratory (Kastman et al., 2016; Wolfe et al., 2014; Wolfe and Dutton, 2015). This olfactory observation piqued our interest because indole has been shown to affect the growth of eukaryotic hosts (Lee et al., 2015), and recent studies of human gut epithelial cells have demonstrated that indole can alter the activity of ion channels (Chimerel et al., 2012), key cellular components that play roles in planarian regeneration and patterning (Beane et al., 2013, 2011; Nogi et al., 2009). Given the potential for indole to impact planarian regeneration, we determined if bacteria in the *D. japonica* microbiome could produce indole and whether bacteria-produced indole can help explain the observed delays in *D. japonica* regeneration.

Bacteria produce indole through degradation of tryptophan via the enzyme tryptophanase (TnaA) (Lee and Lee, 2010; Snell, 1975). To confirm whether bacteria endogenous to the worm microbiome are capable of producing indole, we queried annotations of draft genomes and used BLASTp searches with the *E. coli* *tnaA* sequence for *tnaA* homologs. Genomes of *Aquitalea* sp. FJL05 and *Chryseobacterium* sp. KBW03 contained *tnaA* homologs with 44%–49% amino acid identity to the reference *E. coli* *tnaA* gene (Figure S5). To confirm that these bacteria produce indole, each isolate was grown in tryptophan broth and indole concentrations in broth supernatants were measured using the hydroxylamine-based indole assay, a colorimetric assay with high specificity for indole (Darkoh et al., 2015). After 2 days of incubation, *Aquitalea* sp. FJL05 and *Chryseobacterium* sp. KBW03 produced on average 200 and 40 μ M of indole, respectively (Figure 4A). *Escherichia coli* strain BW25113, a bacterium known to produce indole (Lee and Lee, 2010), was used as a positive control and produced on average 550 μ M indole

in tryptophan broth. An isogenic $\Delta tnaA$ strain from the Keio collection (JW3686-7) was used as a negative control and did not produce detectable levels of indole. In addition, two bacterial species endogenous to the worm microbiome but lacking the *tnaA* gene (Oxalobacteraceae sp. KBW02 and *Variovorax* sp. KBW07) did not produce indole.

To determine whether indole can inhibit worm regeneration, trunk fragments were submerged in sterile water with or without 100 μM pure indole. This concentration of indole was used because higher concentrations were toxic, lower concentrations exhibited weak phenotypes, and 100 μM was within the range produced by bacteria in this system when cultured in a tryptophan broth. Control worm fragments developed visible blastemas by 3 days post-amputation, whereas worms exposed to indole failed to develop typical blastemas at either wound site (Figure 4B). By 5 days post-amputation, eye spots were visible at the anterior end of control worms, whereas worm fragments regenerating in indole still lacked an anterior blastema (and, consequently, lacked eye spots). We removed worm fragments from the indole treatment after 7 days, and they were able to fully regenerate over the course of 14 days in plain water. These results suggest that indole can significantly delay *D. japonica* regeneration without any obvious signs of tissue degeneration or necrosis, similar to the delay that is observed with live bacteria (*Aquitalea* sp. FJL05 and *Chryseobacterium* sp. KBW03).

We next tested whether bacteria-derived indole could also inhibit worm regeneration. Using the same worm regeneration screen approach described above, we tracked the regenerative progress of trunk fragments in the presence of a bacterial inoculum, both with and without the addition of tryptophan, as exogenous tryptophan concentrations control the production of indole in bacteria containing the *tnaA* gene (Li and Young, 2013). As a negative control for the addition of both bacteria and tryptophan, trunk fragments were monitored for regeneration in sterile water with and without tryptophan. As a negative bacterial control, we utilized two bacteria that do not produce indole: Oxalobacteraceae sp. KBW02 and the $\Delta tnaA$ *E. coli* strain JW3686-7 (Figure 4A). Because *Aquitalea* sp. FJL05 was observed to be robust in the production of indole and strongly affected worm regeneration, all downstream analyses utilize *Aquitalea* sp. FJL05 inoculum. We used a lower concentration of bacterial inoculum in these experiments (OD_{600} of 0.3 instead of 2.7 used in the initial bacterial screen above) because preliminary experiments indicated that the addition of tryptophan with higher inoculum densities produced toxic levels of indole killing all worm fragments within 2 days.

Regeneration was significantly delayed in *Aquitalea* sp. FJL05 inoculum supplemented with tryptophan, compared with both the water controls and the *Aquitalea* inoculum alone. By 4 days post-amputation, trunk fragments treated in *Aquitalea* + tryptophan lacked developing tissue near sites of amputation and thus did not develop eye spots, as opposed to worms treated with water or with the *Aquitalea* inoculum alone (Figures 4C–4E). In this experiment, all worms treated with the *Aquitalea* inoculum developed eye spots by 4 days post-amputation, which is in contrast to what we observed in the experiment described in Figure 3B. This seemingly contradictory result can be attributed to the lower concentration of *Aquitalea* used in tryptophan supplementation experiments. Trunk fragments regenerating in the *Aquitalea* + tryptophan treatment were able to successfully regenerate once transferred from the inoculum to sterile worm water (Figure 4E). Trunk fragments regenerating in the *E. coli* strain BW25113-positive control inoculum died, likely because the high concentrations of indole produced with the supplemental tryptophan were toxic. The observed regenerative delay reported for the *Aquitalea* + tryptophan inoculum was not observed in the negative bacterial controls (i.e., Oxalobacteraceae sp. KBW02 or $\Delta tnaA$ *E. coli* JW3686-7), where, regardless of tryptophan concentrations, indole concentrations were below the level of detection (Figure S6).

DISCUSSION

Despite the long use of planaria as models for regeneration, the microbiomes of these animals are poorly characterized. In this study, we describe the diversity of bacteria associated with *D. japonica* and demonstrate that individual bacterial isolates from the *D. japonica* microbiome can mediate regeneration outcomes. High-throughput sequencing and culturing demonstrated that laboratory-reared *D. japonica* worms host a set of bacteria that are consistently observed across individuals and over time, although the relative abundance of individual taxa can vary across individuals. The tractability of the planarian microbiome was demonstrated by our ability to culture many of the dominant bacteria in our 16S rRNA gene amplicon survey. The composition of an established planarian microbiome shows a degree of stability and resistance, as transient exogenous bacteria are unable to colonize and persist after introduction. The consistency of the *D. japonica* microbiome and resistance to invasion suggests that there are host- or bacteria-

derived factors that determine the bacterial community associated with planarians. Indeed, previous studies have identified host immune genes and pathways that eliminate pathogenic bacteria, preventing them from colonizing planarians (Abnave et al., 2014; Pang et al., 2017; Tsoumpta et al., 2017).

Across laboratories, the microbiome composition of laboratory-reared *D. japonica* from the same genetic background were generally similar, with enrichment of certain taxa driving differences between samples. For example, *Aquitalea* sp. was observed in nearly all samples across universities, but was especially high in worms from the University of Minnesota. Colony maintenance practices and rearing conditions (i.e., food and water sources, colony temperature, etc.) differ between laboratories, likely contributing to the observed difference in microbiome composition of laboratory-reared worms. Work in other animal systems has demonstrated that host diet, antibiotic use, and temperature can alter the composition of host-associated microbial communities (Ramsby et al., 2018; Spor et al., 2011; Reese and Dunn 2018). Several taxa identified in this study (e.g., *Rhodoferax* sp., *Pedobacter* sp., *Chryseobacterium* sp., *Pseudomonas* sp., *Acidovorax* sp., and *Oxalobacteraceae* sp.) have previously been reported in the *S. mediterranea* microbiome, a close relative of *D. japonica* (Arnold et al., 2016). These observations suggest that certain bacterial taxa are shared across flatworms in the Dugesiidae family.

Previous work describing microbial impacts on metazoan tissue regeneration and remodeling has largely focused on just a few microbial taxa. A recent study demonstrated that three bacterial species endogenous to *S. mediterranea* (e.g., *Chryseobacterium* sp., *Pseudomonas* sp., and *Vogesella* sp.) can impede host regeneration (Arnold et al., 2016). In the study, the authors identify specific immune genes in the host (e.g., TAK1/MMK/p38) that are sufficient for eliciting regenerative responses in the presence of *Pseudomonas* sp. Our work builds on this previous study of planarian regeneration by screening a larger diversity of bacterial isolates on a different planarian species. We identified bacteria endogenous to the planarian microbiome that can alter regeneration dynamics, ranging from no effect to significant delays in host regeneration. For example, *Acidovorax* sp. FJL06 and *Oxalobacteraceae* sp. KBW02 showed no effect, whereas other bacterial species (e.g., *Aquitalea* sp. FJL05, *Pedobacter* sp. KBW01PK, *Pedobacter* sp. KBW06S, *Pseudomonas* sp. KBW05, *Pacibacter* sp. KBW04, *Variovorax* sp. KBW07, *Chryseobacterium* sp. KBW03, and *Taibaiella* sp. KBW10) were observed to delay and/or alter the host morphology at certain stages of regeneration. These results not only identify specific bacteria of the planarian microbiome that alter host regenerative processes but also demonstrate that bacteria can affect different hallmark features of planarian regeneration (i.e., eye spot development and tissue remodeling). The precise molecular mechanisms that govern atypical regenerative outcomes in the presence of certain bacteria are unclear, but future work will utilize the findings reported in this study to elucidate microbe-host interactions during host regeneration.

Our experiments focusing on indole provide a potential mechanism for microbial mediation of planarian regeneration. Two bacterial species endogenous to *D. japonica* are capable of producing indole (*Aquitalea* sp. FJL05 and *Chryseobacterium* sp. KBW03). Worms regenerating in pure indole suffer substantial inhibition of tissue regeneration. This observation is recapitulated with worms regenerating in an *Aquitalea* sp. inoculum supplemented with tryptophan. In the absence of an indole-producing bacterium or the metabolite tryptophan, worm regeneration proceeds normally. Multiple studies have provided evidence that indole and indole derivatives inhibit cell proliferation in various human cell lines (Frydoonfar et al., 2002; Ping et al., 2011; Telang et al., 1997; Wu et al., 2005). Our work suggests that the established antiproliferative properties of indole and indole derivatives extend to planarian cells, resulting in the inhibition of tissue regeneration that we observed in worms that were exposed to indole. Collectively, our results suggest that bacteria-derived indole can inhibit planarian tissue regeneration, an observation that supports the hypothesis that bacteria play a role in planarian regeneration beyond infection.

Limitations of the Study

We acknowledge that the bacterial enrichment approach that we used in this study has limitations in terms of relevance to natural planarian populations and bacterial community complexity. The bacterial densities used in our study and in Arnold et al. (2016) are higher than what worms may experience in natural conditions. However, the high-density screens are a useful first approach to discover bacteria that have the potential to shape outcomes of regeneration and the possible mechanisms underlying these host-microbe interactions. These coarse-scale observations serve as platform for future fine-scale analyses at the molecular level. The high-density enrichment approach also provides opportunities to develop endogenous bacteria to deliver specific metabolites or genetic constructs in a manner similar

to how *E. coli* is used for RNAi in planarians (Newmark et al., 2003). Our enrichment approach used single species of bacteria so that we could enrich for individual bacterial species in each treatment. Combinations of bacterial species that make up the *D. japonica* may produce different metabolites compared with when grown alone, and future work using multispecies inocula may identify additional bacterial metabolites that mediate regeneration.

Another question that remains to be fully answered is whether planarians experience high enough levels of indole to impact regeneration in either a laboratory or the natural environment. We induced high indole concentrations (>200 μM) in the presence of *Aquitalea* by providing supplemental tryptophan in the worm water. Much higher indole concentrations have been detected in other microbial systems such as the human gut (Darkoh et al., 2015), but it is not known what concentrations planarians naturally experience. Many planarian worms are fed calf or chicken liver when maintained in the laboratory. Liver contains significant amounts of tryptophan (Kuiken et al., 1947) and may provide sufficient levels to stimulate indole production. We are unaware of studies that have quantified indole concentrations in natural aquatic habitats where planarian worms are found.

High concentrations of indole may not be necessary to impact regenerating tissue as localized and lower concentrations of indole may affect regenerative processes at the cellular level. We are currently investigating whether lower concentrations of indole can be detected within planarian tissue to better understand the fine-scale spatial dynamics of indole production in this system. Future studies aim to link these metabolite profiles with the spatial distribution of *Aquitalea* and localized molecular processes that may impact planarian regeneration.

METHODS

All methods can be found in the accompanying *Transparent Methods* supplemental file.

DATA AND SOFTWARE AVAILABILITY

Whole-genome sequences of bacteria isolated from the *Dugesia japonica* microbiome have been deposited in NCBI as QAJI00000000-QAJS00000000 (see Table S2). 16S rRNA amplicon sequence data have been deposited in the NCBI Sequence Read Archive as study accession number SRP141656. Metatranscriptomic sequences have been deposited in MG-RAST with as mgm4738201.3, mgm4738254.3, and mgm4737888.3 (See Table S4).

SUPPLEMENTAL INFORMATION

Supplemental Information includes *Transparent Methods*, seven figures, and six tables and can be found with this article online at <https://doi.org/10.1016/j.isci.2018.11.021>.

ACKNOWLEDGMENTS

Casey Cosetta, Patrick Kearns, and Johanna Bischof provided very helpful feedback on earlier versions of this manuscript. Erik Kastman provided support with data management and bioinformatic analyses. Joshua Finkelstein provided logistical and administrative support. This should read "This research was supported by the Allen Discovery Center program through The Paul G. Allen Frontiers Group (12171).

AUTHOR CONTRIBUTIONS

B.E.W. and M.L. developed and supervised the research project. F.J.L., K.B.W., M.L., and B.E.W. designed the experiments. F.J.L. and K.B.W. executed the experiments. F.J.L., K.B.W., and B.E.W. analyzed data, created figures, and wrote the manuscript.

DECLARATION OF INTERESTS

The authors declare no competing financial interests.

Received: September 14, 2018

Revised: October 31, 2018

Accepted: November 12, 2018

Published: December 21, 2018

REFERENCES

- Abnave, P., Mottola, G., Gimenez, G., Boucherit, N., Trouplin, V., Torre, C., Conti, F., Ben Amara, A., Lepolard, C., Djian, B., et al. (2014). Screening in planarians identifies MORN2 as a key component in LC3-associated phagocytosis and resistance to bacterial infection. *Cell Host Microbe* 16, 338–350.
- Aboobaker, A.A. (2011). Planarian stem cells: a simple paradigm for regeneration. *Trends Cell Biol.* 21, 304–311.
- Agata, K., and Watanabe, K. (1999). Molecular and cellular aspects of planarian regeneration. *Semin. Cell Dev. Biol.* 10, 377–383.
- Álvarez-Presas, M., Baguñà, J., and Riutort, M. (2008). Molecular phylogeny of land and freshwater planarians (Tricladida, Platyhelminthes): from freshwater to land and back. *Mol. Phylogenetic Evol.* 47, 555–568.
- Arnold, C.P., Merryman, M.S., Harris-Arnold, A., McKinney, S.A., Seidel, C.W., Loethen, S., Proctor, K.N., Guo, L., and Sánchez Alvarado, A. (2016). Pathogenic shifts in endogenous microbiota impede tissue regeneration via distinct activation of TAK1/MKK/p38. *Elife* 5, <https://doi.org/10.7554/elife.16793>.
- Beane, W.S., Morokuma, J., Adams, D.S., and Levin, M. (2011). A chemical genetics approach reveals H,K-ATPase-mediated membrane voltage is required for planarian head regeneration. *Chem. Biol.* 18, 77–89.
- Beane, W.S., Morokuma, J., Lemire, J.M., and Levin, M. (2013). Bioelectric signaling regulates head and organ size during planarian regeneration. *Development* 140, 313–322.
- Bely, A.E., and Nyberg, K.G. (2010). Evolution of animal regeneration: re-emergence of a field. *Trends Ecol. Evol.* 25, 161–170.
- Brestoff, J.R., and Artis, D. (2013). Commensal bacteria at the interface of host metabolism and the immune system. *Nat. Immunol.* 14, 676–684.
- Brockes, J.P., and Kumar, A. (2008). Comparative aspects of animal regeneration. *Annu. Rev. Cell Dev. Biol.* 24, 525–549.
- Brockes, J.P., and Kumar, A. (2005). Appendage regeneration in adult vertebrates and implications for regenerative medicine. *Science* 310, 1919–1923.
- Chimerel, C., Field, C.M., Piñero-Fernandez, S., Keyser, U.F., and Summers, D.K. (2012). Indole prevents *Escherichia coli* cell division by modulating membrane potential. *Biochim. Biophys. Acta* 1818, 1590–1594.
- Darkoh, C., Chappell, C., Gonzales, C., and Okhuysen, P. (2015). A rapid and specific method for the detection of indole in complex biological samples. *Appl. Environ. Microbiol.* 81, 8093–8097.
- Durant, F., Lobo, D., Hammelman, J., and Levin, M. (2016). Physiological controls of large-scale patterning in planarian regeneration: a molecular and computational perspective on growth and form. *Regeneration* 3, 78–102.
- Edwards, R., and Harding, K.G. (2004). Bacteria and wound healing. *Curr. Opin. Infect. Dis.* 17, 91–96.
- Eming, S.A., Martin, P., and Tomic-Canic, M. (2014). Wound repair and regeneration: mechanisms, signaling, and translation. *Sci. Transl. Med.* 6, 265sr6.
- Emmons-Bell, M., Durant, F., Hammelman, J., Bessonov, N., Volpert, V., Morokuma, J., Pinet, K., Adams, D.S., Pietak, A., Lobo, D., and Levin, M. (2015). Gap junctional blockade stochastically induces different species-specific head anatomies in genetically wild-type *Girardia dorotocephala* flatworms. *Int. J. Mol. Sci.* 16, 27865–27896.
- Frydoonfar, H.R., McGrath, D.R., and Spigelman, A.D. (2002). Inhibition of proliferation of a colon cancer cell line by indole-3-carbinol. *Colorectal Dis.* 4, 205–207.
- Gentile, L., Cebrià, F., and Bartscherer, K. (2011). The planarian flatworm: an *in vivo* model for stem cell biology and nervous system regeneration. *Dis. Model. Mech.* 4, 12–19.
- Hayes, M.J. (2017). Sulphated glycosaminoglycans support an assortment of planarian rhabdite structures. *Biol. Open* 6, 571–581.
- Holstein, T.W., Hobmayer, E., and Technau, U. (2003). Cnidarians: an evolutionarily conserved model system for regeneration? *Dev. Dyn.* 226, 257–267.
- Kastman, E.K., Kamelamelia, N., Norville, J.W., Cosetta, C.M., Dutton, R.J., and Wolfe, B.E. (2016). Biotic interactions shape the ecological distributions of *Staphylococcus* species. *MBio* 7, <https://doi.org/10.1128/mBio.01157-16>.
- Koppel, N., and Balskus, E.P. (2016). Exploring and understanding the biochemical diversity of the human microbiota. *Cell Chem. Biol.* 23, 18–30.
- Kuiken, K.A., Lyman, C.M., and Hale, F. (1947). The tryptophan content of meat. *J. Biol. Chem.* 171, 561–564.
- Lander, R., and Petersen, C.P. (2016). Wnt, Ptk7, and FGFR expression gradients control trunk positional identity in planarian regeneration. *Elife* 5, <https://doi.org/10.7554/elife.12850>.
- Lee, J.-H., and Lee, J. (2010). Indole as an intercellular signal in microbial communities. *FEMS Microbiol. Rev.* 34, 426–444.
- Lee, J.-H., Wood, T.K., and Lee, J. (2015). Roles of indole as an interspecies and interkingdom signaling molecule. *Trends Microbiol.* 23, 707–718.
- Lee, Y.K., and Mazmanian, S.K. (2010). Has the microbiota played a critical role in the evolution of the adaptive immune system? *Science* 330, 1768–1773.
- Li, G., and Young, K.D. (2013). Indole production by the tryptophanase TnaA in *Escherichia coli* is determined by the amount of exogenous tryptophan. *Microbiology* 159, 402–410.
- Lobo, D., Beane, W.S., and Levin, M. (2012). Modeling planarian regeneration: a primer for reverse-engineering the worm. *PLoS Comput. Biol.* 8, e1002481.
- Lobo, D., and Levin, M. (2015). Inferring regulatory networks from experimental morphological phenotypes: a computational method reverse-engineers planarian regeneration. *PLoS Comput. Biol.* 11, e1004295.
- McFall-Ngai, M., Hadfield, M.G., Bosch, T.C.G., Carey, H.V., Domazet-Lošo, T., Douglas, A.E., Dubilier, N., Eberl, G., Fukami, T., Gilbert, S.F., et al. (2013). Animals in a bacterial world, a new imperative for the life sciences. *Proc. Natl. Acad. Sci. U S A* 110, 3229–3236.
- Miller, C.A., Johnson, W.H., Millis, S.C. (1955). The sterilization and preliminary attempts in the axenic cultivation of the black planarian *Dugesia* *orocephala*, In: *Proceedings of the Indiana Academy of Science*. pp. 237–242.
- Morgan, T.H. (1898). Experimental studies of the regeneration of *Planaria maculata*. *Roux's Arch. Dev. Biol.* 7, 364–397.
- Morokuma, J., Durant, F., Williams, K.B., Finkelstein, J.M., Blackiston, D.J., Clements, T., Reed, D.W., Roberts, M., Jain, M., Kimel, K., et al. (2017). Planarian regeneration in space: Persistent anatomical, behavioral, and bacteriological changes induced by space travel. *Regeneration (Oxf)* 4, 85–102.
- Newmark, P.A., Reddien, P.W., Cebrià, F., and Sánchez Alvarado, A. (2003). Ingestion of bacterially expressed double-stranded RNA inhibits gene expression in planarians. *Proc. Natl. Acad. Sci. U S A* 100 (Suppl 1), 11861–11865.
- Nogi, T., Zhang, D., Chan, J.D., and Marchant, J.S. (2009). A novel biological activity of praziquantel requiring voltage-operated Ca²⁺ channel beta subunits: subversion of flatworm regenerative polarity. *PLoS Negl. Trop. Dis.* 3, e464.
- Oviedo, N.J., Newmark, P.A., and Sánchez Alvarado, A. (2003). Allometric scaling and proportion regulation in the freshwater planarian *Schmidtea mediterranea*. *Dev. Dyn.* 226, 326–333.
- Pang, Q., Gao, L., Bai, Y., Deng, H., Han, Y., Hu, W., Zhang, Y., Yuan, S., Sun, W., Lu, Y., et al. (2017). Identification and characterization of a novel multifunctional placenta specific protein 8 in *Dugesia japonica*. *Gene* 613, 1–9.
- Pedersen, K.J. (1963). Slime-secreting cells of planarians. *Ann. N. Y. Acad. Sci.* 106, 424–443.
- Petersen, C.P., and Reddien, P.W. (2008). Smed-βcatenin-1 is required for anteroposterior blastema polarity in planarian regeneration. *Science* 319, 327–330.
- Ping, J., Li, J.-T., Liao, Z.-X., Shang, L., and Wang, H. (2011). Indole-3-carbinol inhibits hepatic stellate cells proliferation by blocking NADPH oxidase/reactive oxygen species/p38 MAPK pathway. *Eur. J. Pharmacol.* 650, 656–662.

- Postler, T.S., and Ghosh, S. (2017). Understanding the holobiont: how microbial metabolites affect human health and shape the immune system. *Cell Metab.* 26, 110–130.
- Ramsby, B.D., Hoogenboom, M.O., Whalan, S., and Webster, N.S. (2018). Elevated seawater temperature disrupts the microbiome of an ecologically important bioeroding sponge. *Mol. Ecol.* 27, 2124–2137.
- Reddien, P.W., and Sánchez Alvarado, A. (2004). Fundamentals of planarian regeneration. *Annu. Rev. Cell Dev. Biol.* 20, 725–757.
- Reese, A.T., and Dunn, R.R. (2018). Drivers of microbiome biodiversity: a review of general rules, feces, and ignorance. *MBio* 9, <https://doi.org/10.1128/mBio.01294-18>.
- Sampson, T.R., and Mazmanian, S.K. (2015). Control of brain development, function, and behavior by the microbiome. *Cell Host Microbe* 17, 565–576.
- Sánchez Alvarado, A. (2000). Regeneration in the metazoans: why does it happen? *Bioessays* 22, 578–590.
- Sánchez Alvarado, A., and Tsonis, P.A. (2006). Bridging the regeneration gap: genetic insights from diverse animal models. *Nat. Rev. Genet.* 7, 873–884.
- Sannino, D.R., Dobson, A.J., Edwards, K., Angert, E.R., and Buchon, N. (2018). The *Drosophila melanogaster* gut microbiota provisions thiamine to its host. *MBio* 9, <https://doi.org/10.1128/mBio.00155-18>.
- Scimone, M.L., Cote, L.E., and Reddien, P.W. (2017). Orthogonal muscle fibres have different instructive roles in planarian regeneration. *Nature* 551, 623–628.
- Sharon, G., Garg, N., Debelius, J., Knight, R., Dorrestein, P.C., and Mazmanian, S.K. (2014). Specialized metabolites from the microbiome in health and disease. *Cell Metab.* 20, 719–730.
- Snell, E.E. (1975). Tryptophanase: structure, catalytic activities, and mechanism of action. *Adv. Enzymol. Relat. Areas Mol. Biol.* 42, 287–333.
- Spor, A., Koren, O., and Ley, R. (2011). Unravelling the effects of the environment and host genotype on the gut microbiome. *Nat. Rev. Microbiol.* 9, 279–290.
- Tanaka, E.M., and Reddien, P.W. (2011). The cellular basis for animal regeneration. *Dev. Cell* 21, 172–185.
- Telang, N.T., Katdare, M., Bradlow, H.L., Osborne, M.P., and Fishman, J. (1997). Inhibition of proliferation and modulation of estradiol metabolism: novel mechanisms for breast cancer prevention by the phytochemical indole-3-carbinol. *Proc. Soc. Exp. Biol. Med.* 216, 246–252.
- Tettamanti, G., Saló, E., González-Estévez, C., Felix, D.A., Grimaldi, A., and de Egileor, M. (2008). Autophagy in invertebrates: insights into development, regeneration and body remodeling. *Curr. Pharm. Des.* 14, 116–125.
- Tsoumtsa, L.L., Torre, C., Trouplin, V., Coiffard, B., Gimenez, G., Mege, J.-L., and Ghigo, E. (2017). Antimicrobial capacity of the freshwater planarians against *S. aureus* is under the control of timeless. *Virulence* 8, 1160–1169.
- Vuong, H.E., Yano, J.M., Fung, T.C., and Hsiao, E.Y. (2017). The microbiome and host behavior. *Annu. Rev. Neurosci.* 40, 21–49.
- Wolfe, B.E., Button, J.E., Santarelli, M., and Dutton, R.J. (2014). Cheese rind communities provide tractable systems for *in situ* and *in vitro* studies of microbial diversity. *Cell* 158, 422–433.
- Wolfe, B.E., and Dutton, R.J. (2015). Fermented foods as experimentally tractable microbial ecosystems. *Cell* 161, 49–55.
- Wong, A.C.-N., Dobson, A.J., and Douglas, A.E. (2014). Gut microbiota dictates the metabolic response of *Drosophila* to diet. *J. Exp. Biol.* 217, 1894–1901.
- Wu, H.-T., Lin, S.-H., and Chen, Y.-H. (2005). Inhibition of cell proliferation and *in vitro* markers of angiogenesis by indole-3-carbinol, a major indole metabolite present in cruciferous vegetables. *J. Agric. Food Chem.* 53, 5164–5169.

ISCI, Volume 10

Supplemental Information

The Bacterial Metabolite Indole Inhibits

Regeneration of the Planarian

Flatworm *Dugesia japonica*

Fredrick J. Lee, Katherine B. Williams, Michael Levin, and Benjamin E. Wolfe

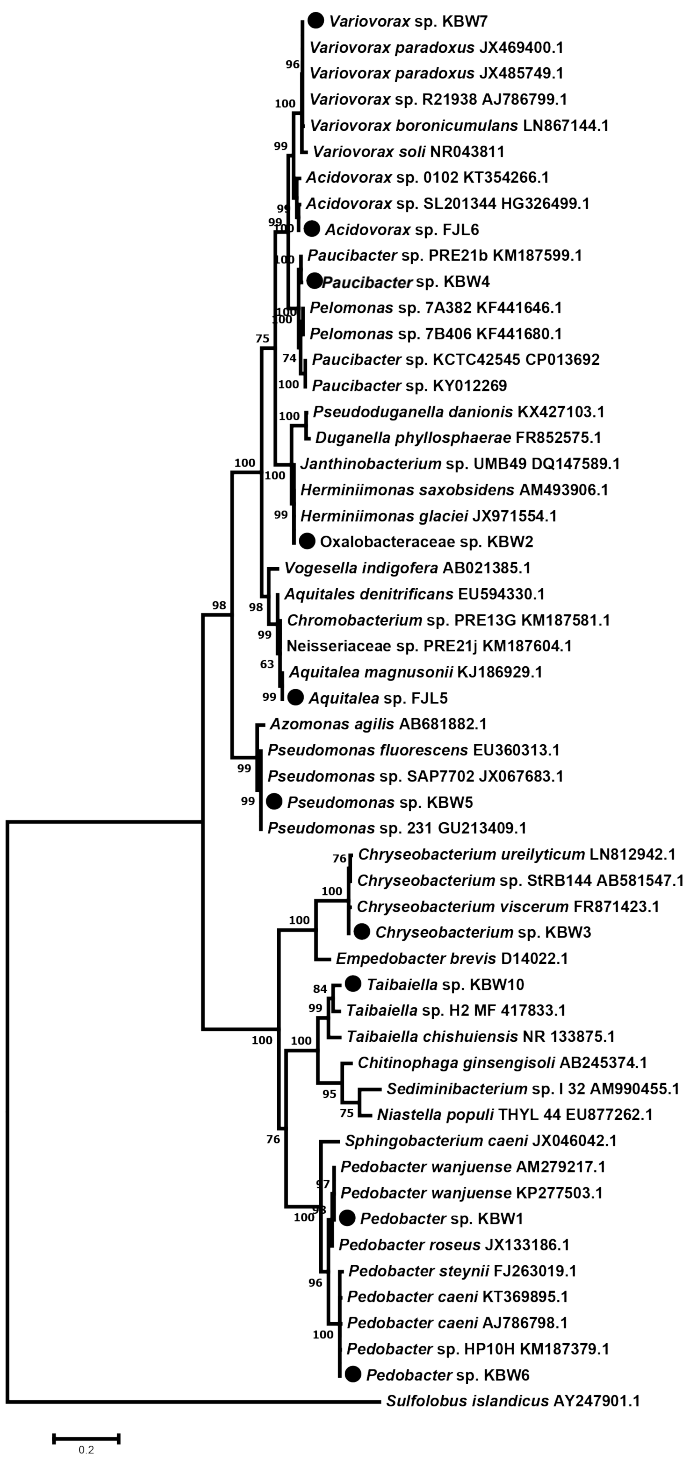


Figure S1. Phylogenetic tree of the 16S rRNA gene of bacteria cultured from the *Dugesia japonica* microbiome, related to Figure 1. 16S rRNA sequences of *D. japonica* isolates (indicated with circles) and reference sequences from NCBI were aligned using Mothur V1.35.1: (align.seq (reference = SILVA ribosomal database) and a maximum likelihood phylogeny of the 16S rRNA gene was constructed in MEGA v 7.0.26 (default settings with G+I and 1000 bootstraps).

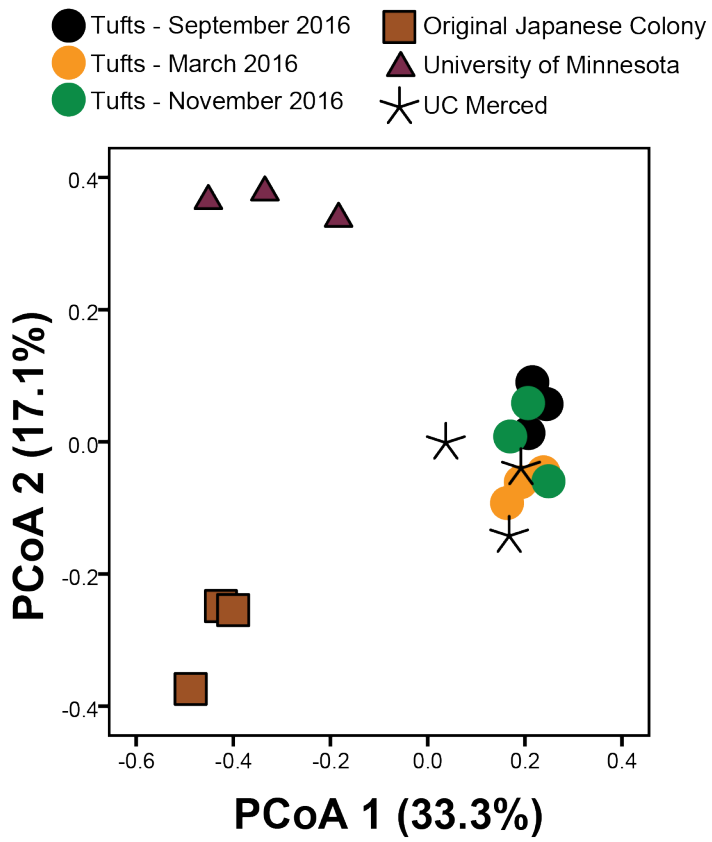


Figure S2. Principal coordinate analysis of Bray-Curtis dissimilarity from the 16S rRNA survey of *Dugesia japonica* across different labs (Data; Figure 1D), related to Figure 1E-D. Bray-Curtis calculations and PCoA were performed in Mothur V1.35.1 with default settings.

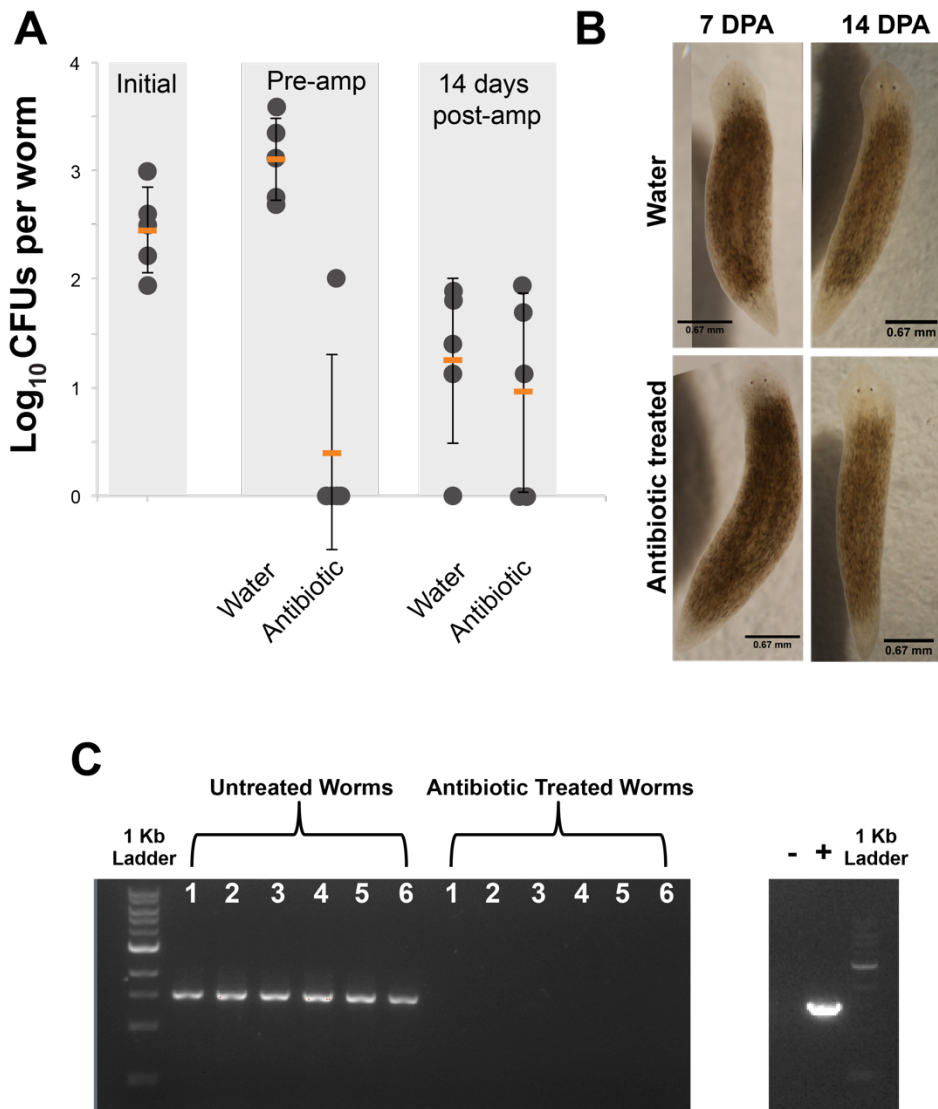


Figure S3. Antibiotic treatment depletes the bacterial load in *Dugesia japonica* without visible effects on host regeneration, related to Figure 3. From a cohort of worms ($n = 25$), five worms were sampled individually to determine the initial bacterial load by destructive sampling (“Initial” in A). Remaining worms were subdivided into sterile worm water with or without antibiotics (1.0 mg/mL of erythromycin and 0.1 mg/mL ciprofloxacin, with fresh antibiotics added every three days) for one week. After treatment, worms were washed in sterile worm water three times, trunk fragments aseptically amputated, and fragments were placed in sterile worm water and regeneration was monitored for 14 days. **(A)** Bacterial load as determined by destructively harvesting worms and counting colonies on brain heart infusion agar. Initial = worm bacterial load before treatment. Pre-amp = bacterial load of water control and antibiotic treated worms before amputation. 14-days post amp = bacterial load of water control and antibiotic treated worms after 14 days of regeneration. **(B)** Regeneration of *D. japonica* is not impacted by antibiotic treatment. Heads and tails regenerate in similar manner in both water and antibiotic treated worms. **(C)** PCR with universal bacterial primers (27F/1492R) on DNA extracted from individual worms. DNA extraction and PCR protocol is described in the methods Genomic DNA from *Chryseobacterium* sp. KBW03 was used as the positive control (“+”). PCR water was used as negative control (“-”).

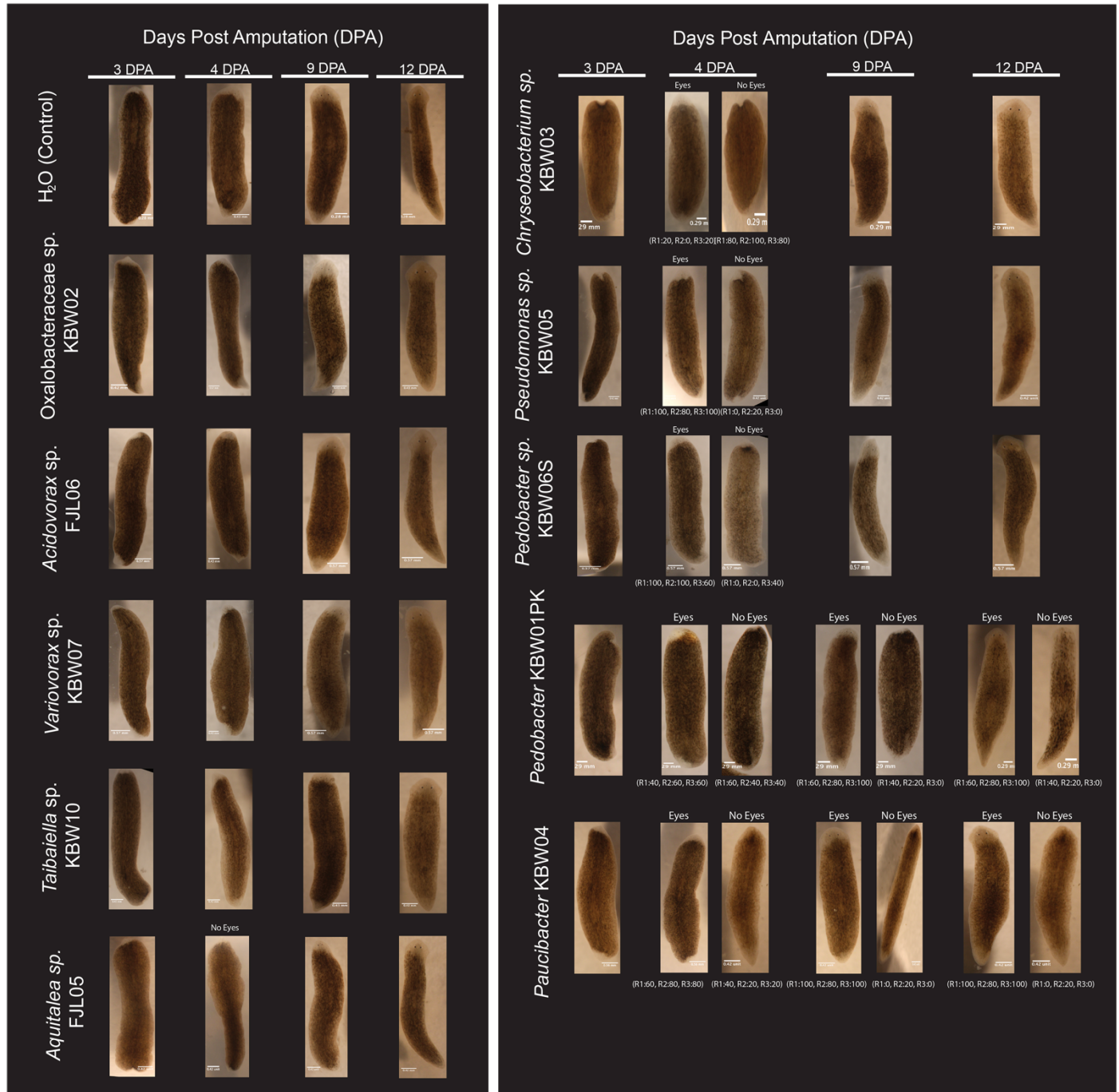


Figure S4. Regeneration screen of bacterial inocula, related to Figure 3. Representative images of the regenerative progress of trunk fragments treated in bacterial inocula or sterile worm water over the course of 12 days. Numbers below images indicate the proportion of observed morphologies for each of the three biological replicates (R1, R2, R3). All images without numbers indicate treatments where all worms displayed the same morphology.

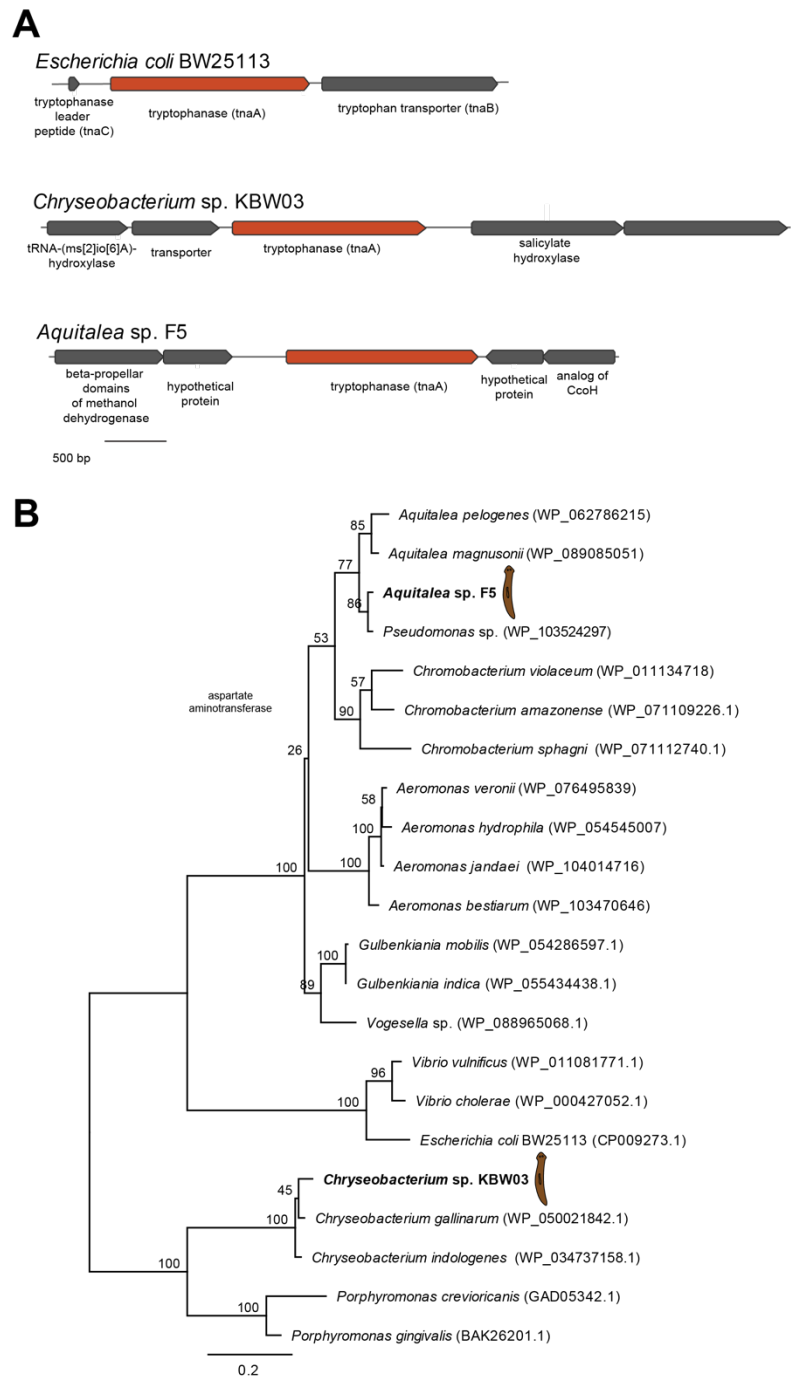


Figure S5. Detection and diversity of tryptophanase genes in bacteria associated with *Dugesia japonica*, related to Figure 4. (A) Overview of the *tnaA* gene in *E. coli* BW25113 and in *Chryseobacterium* sp. KBW03 and *Aquitalea* sp. F5. The *tnaA* gene is highlighted in orange. **(B)** A maximum likelihood phylogeny of an alignment of amino acid sequences of the *tnaA* gene from diverse bacteria and from bacteria isolated from the planarian *Dugesia japonica*. Planarian isolates are indicated with a worm icon. The maximum likelihood phylogeny was created using RAxML with 100 bootstraps and a GAMMA BLOSUM62 protein model.

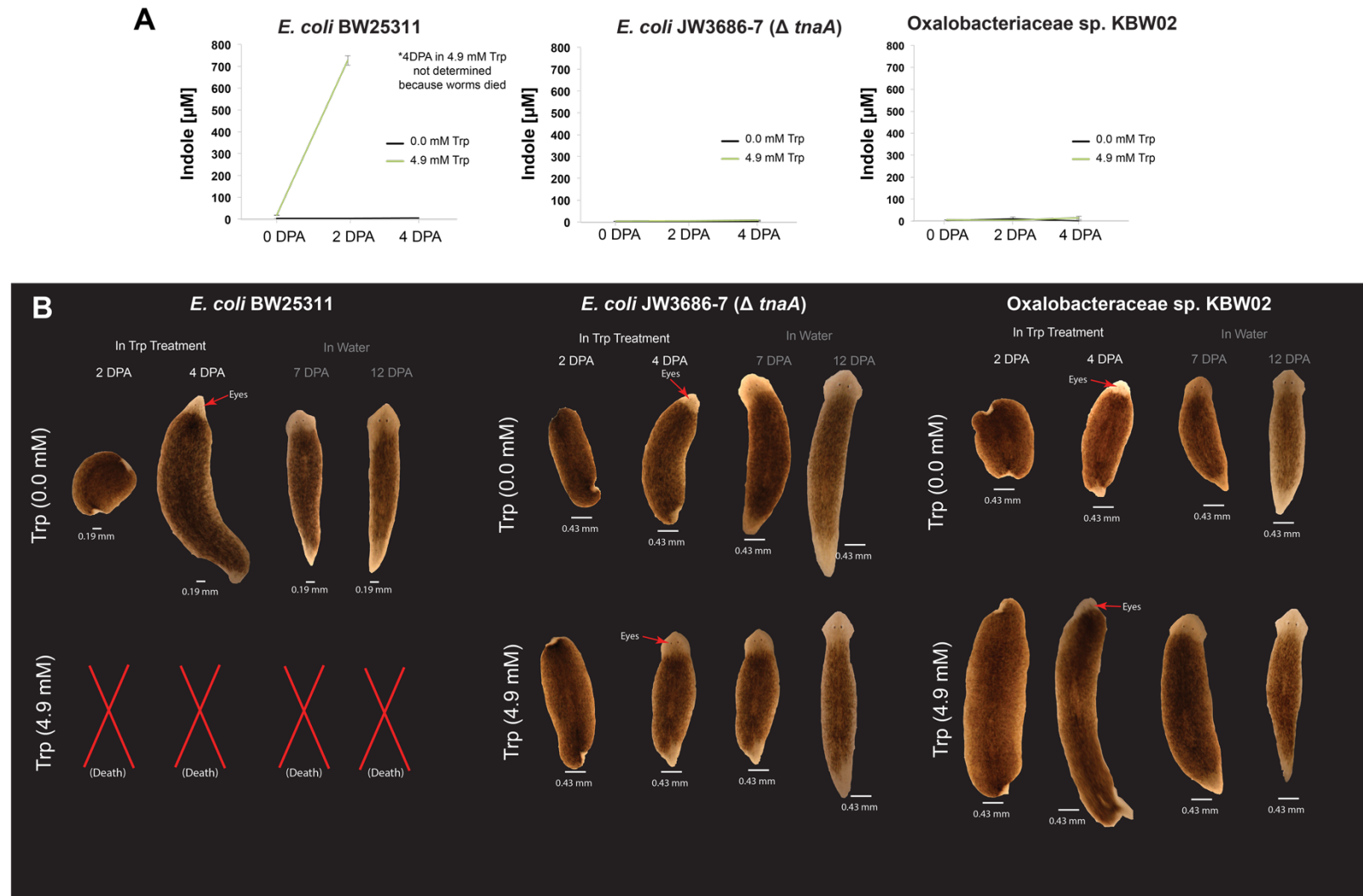


Figure S6. Bacteria that do not produce indole do not delay *D. japonica* regeneration, related to Figure 4. Planarian regeneration screen with pure cultures of *E. coli* BW25311, *E. coli* JW3686-7(Δ *tnaA*) and Oxalobacteraceae sp. KBW02, both with and without tryptophan (0.0 mM and 4.9 mM) were conducted as described in the methods. **(A)** Indole production in bacterial inocula with and without supplemental tryptophan. Lines represent means and error bars represent +/- standard deviation **(B)** Regeneration phenotypes observed in bacterial inocula with and without supplemental tryptophan. For each treatment condition, three biological replicates ($n = 5$ per replicate) were conducted.

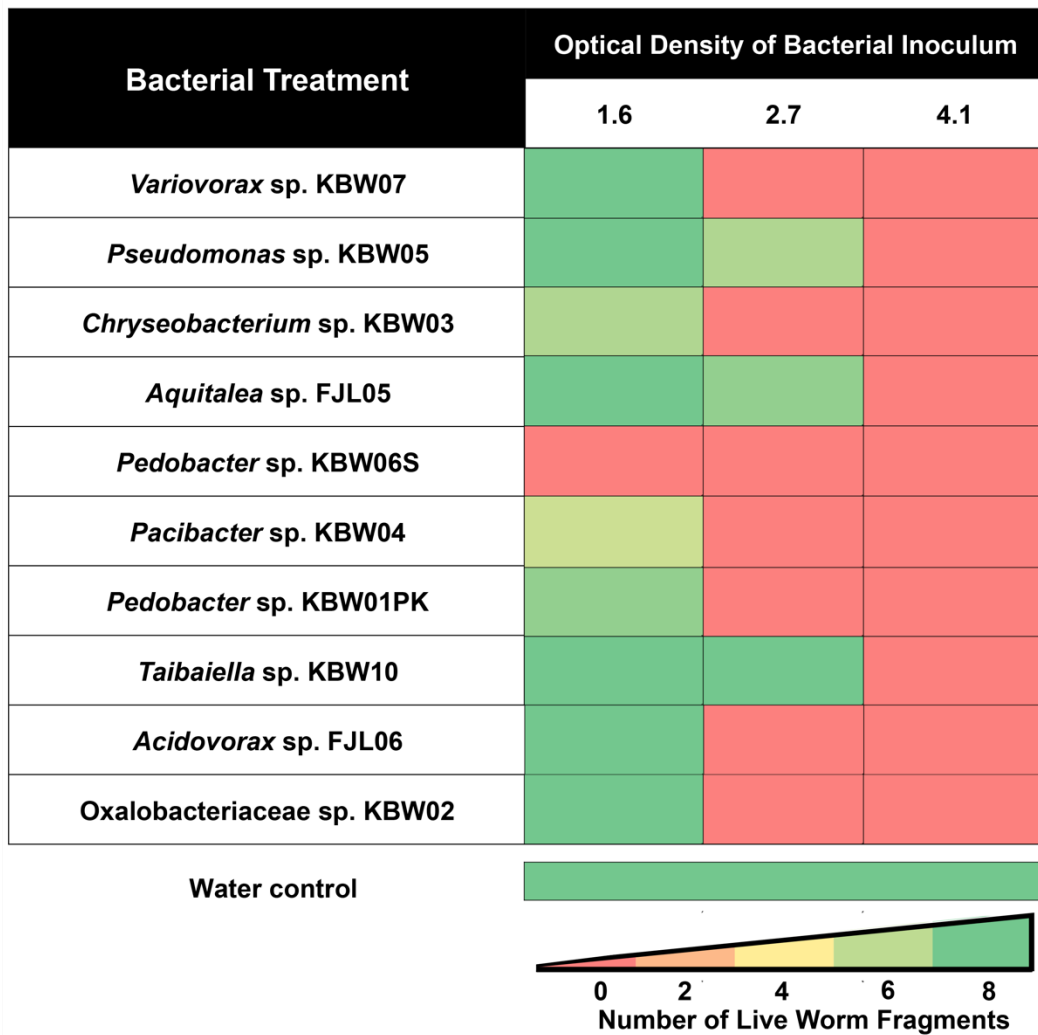


Figure S7. Heat-map of worm survival in different concentration of a bacteria, related to Transparent Methods, related to Figure 3. For each inoculum, eight regenerating trunk fragments were placed in the bacterial suspension at an OD₆₀₀ of 1.6, 2.7, and 4.1. Worm survival was monitored over the course of seven days post amputation (DPA). At seven DPA, the number of live worms were scored from 0 (red) to 8 (Green). Three biological replicates were performed for each inoculum.

TRANSPARENT METHODS

Planarian care

A clonal strain of *Dugesia japonica* (GI) maintained in the Levin laboratory (Tufts University, Boston, MA) was used in all experiments. The colony was established and maintained as previously described (Oviedo et al., 2008) in sterile Poland Springs spring water (hereafter worm water). Planaria used in each experiment measured between 5 mm and 20 mm in length. Worms were starved at least 7 days before each experiment, and continued to starve for the duration of each experiment. Starvation is a common approach used to clear gut contents and to keep water clean before planarian amputation and regeneration. We used this standardized starvation protocol for all of our regeneration experiments. For experiments analyzing microbiome composition of worms from other laboratories, express shipments of the GI strain were obtained from the following locations: Umesono (Dr. Yoshihiko Umesono, Hyogo University, Japan; Dr. Jonathan Merchant of the University of Minnesota, Minneapolis, MN; Dr. Nestor Oviedo, University of California, Merced, CA).

Bacterial strain isolation, taxonomic classification, genome sequencing, and 16S rRNA phylogeny construction

To isolate microbes associated with *D. japonica* reared in the Levin laboratory, 2 - 3 worms were aseptically homogenized in 1x PBS using a sterile micropestle in a 1.5 mL Eppendorf tube. Homogenates were serially diluted in PBS and plated on brain heart infusion (BHI) agar (BD Bacto). All plates were incubated aerobically at room temperature for 7 days. After incubation, representative colonies of distinct morphotypes (colony pigment, margin, and elevation) were isolated, streaked until pure cultures were obtained on BHI agar, and glycerol stocks created. Attempts to culture other microbes on different media types (De Man-Rogosa-Sharp, trypticase soy, potato dextrose, and Reasoner's 2A) did not yield additional microbes. We were also unable to culture microbes on any media types in anaerobic conditions.

To obtain an initial taxonomic identity of the bacterial isolates, colony PCR was conducted by amplifying the 16S rRNA gene with universal bacterial primers 27F and 1492R (Lane, 1991; Turner et al., 1999) using the following PCR mix: 12.5 µL Q5 Hot Start High-fidelity master mix (New England BioLabs), 1 µL of each primer (10 µM), and 9.5 µL molecular grade water. The following thermocycler conditions were used: initial denaturation - 5 min at 98°C; 30 cycles - 10 sec at 98°C, 30 sec at 58°C, 45 sec at 72°C; extension - 2 min at 72°C. Amplified products were purified and sequenced via Sanger sequencing by Genewiz.

Full genomes were obtained from bacterial isolates with unique 16S rRNA sequences. BHI broth cultures were grown at 24 °C for 2 days, cells were harvested via centrifugation, and DNA extracted via the DNeasy PowerSoil kit (Qiagen) using the standard protocol provided by the manufacturer. Approximately 1µg of genomic DNA was used as input for fragmentation and library preparation using the NEBNext Ultra DNA Library prep kit for Illumina (New England Biolabs) as previously described (Kastman et al., 2016). DNA was fragmented to a range of approximately 300-700 base pairs in length by digesting samples with NEBNext dsDNA Fragmentase (New England Biolabs) for 20 minutes. This fragmented DNA was used as the input for the NEBNext Ultra DNA Library prep kit. Genomic libraries were sequenced using paired-end sequencing (125 base pairs in length) on an Illumina HiSeq 2000 at the Harvard FAS Center for Systems Biology. Reads were assembled into contigs using the default *de novo* assembly settings in CLC Genomic Workbench 10. The resulting contigs were annotated with RAST (Aziz et al., 2008). Annotated genomes have been deposited at NCBI (Accession numbers in Table S2).

To determine how our worm bacterial isolates were related to previously characterized bacteria, full length 16S rRNA gene sequences were extracted from the assembled and annotated genomes. Sequences were aligned and classified using the following commands in Mothur (align.seq (reference = SILVA ribosomal database (non-redundant version 132),

classify.seqs (reference and taxonomy = Greengenes ribosomal database (version 13.8)). A 16S rRNA gene phylogeny was constructed by aligning the full length 16S rRNA gene sequences with reference sequences of closely related taxa obtained from NCBI. Sequences were aligned as described above and a maximum likelihood phylogeny of the 16S rRNA gene was constructed in MEGA v 7.0.26 (default settings with G+I and 1000 bootstraps).

DNA extraction, 16S rRNA amplicon library preparation, and data processing

Individual worms of comparable size were rinsed aseptically in 1x PBS twice, transferred to a sterile centrifuge tube with 200 µL of PBS, and homogenized with a sterile pestle. Worms were starved for one week before being processed (see above). To determine the microbiome composition of individual worms, DNA was extracted from homogenates via the DNeasy PowerSoil kit (Qiagen) as described above. 5 ng/µL of DNA was used for construction of barcoded amplicon libraries using primers (F515/R806) that targeted the V4 region of the 16S rRNA gene as previously described (David et al., 2014; Wolfe et al., 2014). The following PCR mix was used: 12.5 µL Q5 Hot Start High-fidelity master mix (New England BioLabs), 1 µL of each primer (10 µM), and 9.5 µL molecular grade water. The following thermocycler conditions were used: initial denaturation - 30 sec at 98°C; 35 cycles - 10 sec at 98°C, 30 sec at 50°C, 45 sec at 72°C; extension - 10 min at 72°C. Multiplexing was performed with 12-base-pair Golay barcodes added to the reverse primer (Caporaso et al., 2011). PCR of each sample was performed in duplicate and duplicate PCR products pooled for each sample were pooled. Approximately equal concentrations of amplicons from each sample were pooled and paired-end Illumina sequencing was performed as described above. Raw data was deposited in the NCBI Sequence Read Archive with study accession number SRP141656.

High quality reads (q30 threshold) were processed using Mothur version 1.35.1 (Schloss et al., 2009) as previously described (Lee et al., 2015). Sequences were classified using a custom ribosomal database that combined the Greengenes database (Version 13.8) with the 16S rRNA gene sequences acquired from the isolates cultured in this study. Sequences were binned into operational taxonomic units (OTUs) based on 97% identity. OTUs present in the PCR negative control libraries were removed from the analysis. Libraries for each sample were subsampled to the smallest sample size (1270 sequences) to normalize results across libraries. OTUs greater than 1% average abundance across all samples are presented in the figures. Bray-Curtis dissimilarities was calculated across samples and depicted by principal coordinate analysis (PCoA) using Mothur.

16S rRNA transcript mining of a *D. japonica* metatranscriptome

Three cohorts of worms (5 worms per cohort) were removed from the Levin lab colony of *D. japonica* strain GI and rinsed in PBS as described above. Worms were aseptically transferred to sterile RNase-free tubes containing 1 mL of Trizol and sterile glass beads with a diameter of 106 - 600 µm. Samples were homogenized twice with a vortexer at max speed for 40 seconds using a MoBio Vortex Adapter. Samples were briefly centrifuged to settle the beads to the bottom of the tube. The supernatant was transferred to a sterile RNase-free 1.5 mL tube and RNA was extracted using Trizol. RNA extracts were resuspended in RNA Storage Solution (Bioline) and stored at -80°C for downstream analysis. To deplete samples of eukaryotic RNAs the Ambion MicroBEnrich kit was utilized as described by Lee et. al., 2015. The integrity and quantity of the RNA was determined via an Agilent 2100 Bioanalyzer using an RNA Nano chip. Samples of high quality were DNase-treated (Turbo DNA-free kit, Invitrogen) to rid samples of contaminating DNA. To confirm the absence of DNA in RNA samples, PCR of the 16S rRNA gene using the 27F/1492R primer set was conducted as previously described. No amplified product was observed when electrophoresis through a 1% agarose gel was performed on the PCR product. DNA-free RNA was stored at -80°C until utilized for library preparation. Libraries were prepared using the NEBNext RNA Ultra II Library Prep Kit (New England Biolabs)

according to the manufacturer's instructions. RNA was fragmented for 15 minutes using heat (94 °C), cDNA synthesized, and libraries size-selected for 300 - 400 bp using Ampure XP beads (Beckman Coulter). cDNA libraries were sequenced using paired-end sequencing as described above.

To obtain a profile of bacteria actively transcribing the 16S rRNA gene, we developed a custom pipeline to mine cDNA libraries for 16S rRNA transcripts (i.e. reads). Initially, high quality reads (q30 threshold) were queried against the *D. japonica* genome (WGS accession MWRL00000000.1) for significant homology (80% similarity across 50% of the length of sequence) using CLC Genomic Workbench 10. After removal of reads that mapped to the host genome, the number of remaining reads ranged from 4,100 to 19,875 sequences across the three libraries. The remaining reads were then queried against a custom rRNA database (described in previous sections) using default read mapping settings in CLC. Reference sequences with at least one mapped read were binned at 97% identity using the full length reference sequences.

To test the accuracy of the pipeline described above, an *in silico* analysis was conducted with a mock 16S rRNA dataset. The mock community dataset was constructed with sequences of 150 base pairs in length. In total 190,000 sequences were used in the dataset, including sequences that span various regions of the 16S rRNA gene from 19 taxa, including sequences from bacteria cultured in this study (**Table S2**) and 9 reference sequences from NCBI (accession numbers indicated): *Dialister* sp. (NR_026229), *Staphylococcus* sp. (CP027422.1), *Erwinia* sp. (AF373200), *Hymenobacter* sp. (FR682729), *Chitinophaga* sp. (MF687748), *Rhodoferax* sp. (MG576020), *Burkholderiales* sp. (EF114435), *Lactobacillus* sp. (LT631756), and *Rhodococcus* sp. (LT984719). The pipeline correctly mapped and classified reads with an average accuracy of 95% +/- 2.0 (**Table S3**). Reads that were misclassified typically mapped to regions of the 16S rRNA gene that were conserved at the family level.

Culture-dependent sampling of the worm microbiome

Throughout the study, two culture-dependent methods were performed to determine bacterial diversity of the worm microbiome. A destructive sampling approach, where worms were sacrificed, was developed to sample all culturable bacteria associated with the worm. A non-destructive method, where worms were kept alive after sampling, was used to sample bacteria loosely associated with the outside surfaces of the worm.

For destructive sampling, worms were briefly rinsed with sterile Poland Springs water. To remove external microbes, individual worms were aseptically transferred into 1.5 mL tube containing 400µL PBS (1x) and the tubes briefly vortexed. Individual worms or amputated fragments were then placed into a sterile 1.5 mL tube containing 400µL PBS (1x), and then homogenized using a sterile micropesle. The homogenate was serially diluted and plated on BHI agar plates that were aerobically incubated at room temperature for 7 days. After incubation, bacterial colonies with similar morphotypes (as described above) were grouped and tallied. One representative colony of each morphotype was selected and colony PCR of the 16S rRNA gene performed with the primers 27F/1492R. The amplified product was sequenced via Sanger sequencing and the identity of each morphotype confirmed by classifying the sequence as described above. The bacterial composition of samples was determined by calculating total colony forming units (CFUs) for each morphotype. The relative abundance of an individual morphotype was determined by calculating the total CFUs across all morphotypes on a single plate and dividing the reported CFUs for a particular morphotype to that of the total.

For non-destructive sampling, whole individual worms or fragments were transferred into a 1.5 mL tube containing 400µL PBS (1x) and then briefly vortexed. The worms were removed from the tube and the remaining PBS solution was serially diluted and plated on BHI agar as described above. Growth conditions and analysis of relative abundance of colony types was performed as described above.

To determine the culturable composition of worm segments (i.e. head, trunk, and tail), destructive sampling was performed on 9 individual worms aseptically amputated above and below the pharynx. To determine the culturable composition of internal and external bacteria associated with *D. japonica*, 9 Individual worms were initially sampled non-destructively to isolate loosely associated bacteria and then destructively to isolate bacteria that were closely associated with the worm or living inside of the worm.

Addition of exogenous microbes experiment

To determine whether exogenous bacteria can be incorporated and maintained in the *D. japonica* microbiome, 60 fully regenerated worms were acquired from the main laboratory colony. To determine the initial composition of the worm microbiome, 10 worms were randomly selected from the group and individual worms sampled destructively. The remaining worms were then subdivided into two groups ($n = 25$, per treatment), where the first group was treated in a bacterial inoculum containing six bacterial isolates: *Escherichia coli* DH5 α (a lab strain), *Chryseobacterium* sp. PW3, *Tsukamurella* sp. F4, *Flavobacterium* sp. PW5, *Arthrobacter* sp. PW6, and *Arthrobacter* sp. A3. Partial 16S rRNA gene sequences of these bacterial strains have been deposited at NCBI under the accession numbers MH795542-MH795546. The second group of worms were placed in sterile worm water. Both treatment groups were incubated at 10°C for the entirety of the experiment.

Prior to the bacterial treatment, pure cultures of each isolate were cultivated in BHI broth using conditions previously described. After 3 days of growth, cells were pelleted by centrifugation (10,000 $\times g$ for 10 minutes). The supernatant was removed and the cells were washed twice in 50 mL of PBS (1x) by resuspending and pelleting cells between washes. Finally, cells were resuspended in sterile worm water and diluted to an OD₆₀₀ of 0.6. A mixed culture was constructed using equal cell densities for all six bacteria in a total volume of 50 mL. 25 worms were added to the cell suspension and maintained at 10°C for three days. The worms were moved to a fresh, sterile Petri dish containing sterile worm water, and the dish was rinsed out five times with sterile water to remove external microbes from the worms. After rinsing, 10 worms were destructively sampled and the remaining 15 were kept in sterile worm water at 10°C. Three days after rinsing, 10 worms were destructively sampled, and the remaining 5 worms were kept in sterile worm water at 10 °C. 15 days after rinsing, the remaining 5 worms were destructively sampled. Worms that were kept in sterile worm water for the entirety of the experiment (control worms) were sampled alongside the exogenous treatment group at identical time points.

Planarian regeneration screen using bacterial enrichments

Prior to the screen, each bacterial isolate was cultivated, harvested, washed, and resuspended in sterile worm water as described above. To determine bacterial cell density, the optical density (OD) was measured at 600 nm. Based on the OD₆₀₀ measurement, bacterial suspensions were diluted to an OD between the range of 1.0 - 2.7, depending on the isolate. For each isolate, the OD selected for the regeneration screen was determined based on a preliminary results where a range of ODs were examined to determine the best bacterial concentration with a minimum of an LD₅₀ at 7 days post amputation (Figure S7). The following ODs were used in our study 1.0 (*Chryseobacterium* sp. KBW03, *Paucibacter* sp. KBW04, and *Pedobacter* sp. KBW06PK), 2.7 (*Aquitalea* sp. FJL05), and 1.6 for all other bacterial inocula. For each inoculum, CFUs/mL were determined by serially diluting the corresponding inoculum, plating a portion of the inoculum on BHI agar, and counting CFUs after incubation (Table S6).

After the inoculum was prepared, the head and tail were aseptically amputated from fully regenerated worms that were previously treated in a week long bacterial cocktail regimen (1.0mg/mL erythromycin and 0.1 mg/mL ciprofloxacin) that was replenishing every 3-4 days. Antibiotic treatment substantially depletes the bacterial load of worms without affecting host

regeneration (**Figure S3**). Trunk fragments treated with the antibiotic cocktail were washed, transferred, and submerged into a bacterial inoculum for 12 days at 20°C. The bacterial inoculum was removed and refreshed once a week. As a negative control and a proxy for standard regeneration, trunk fragments were also placed in sterile worm water and monitored for regenerative outcomes. For each treatment, three biological replicates of 5 fragments were placed in 8 mL of bacterial inoculum or water.

Over the course of 12 days, worms were examined for survival of fragments, eye spot development, and overall body morphology at 2x magnification using a Zeiss Stemi 200-C stereo microscope. Throughout the experiment, representative images were taken for each replicate, with all worms from all treatments imaged on 7 and 12 days post amputation. To determine body length-to-width ratios, images were uploaded to ImageJ and the segment line tool was used to measure both the length and width of regenerating worms. To determine length of a worm fragment, a continuous segment line was drawn following the most centralized region of the worm from head to tail. Body width was measured by drawing a perpendicular line segment across the widest region of the trunk area. Body ratios were determined by dividing the length by the width measurement. Regenerating worms without a defined head and worms that underwent a fissioning event during the experiment were excluded from the analysis. To assess statistical significance of differences in the length-to width ratios of individual time points (i.e. 7 or 12 days post-amputation), bacterial treatments were compared to their respective water control using a Welch's t-test on normally distributed datasets. Post-hoc analysis performed with a Bonferroni correction identified bacterial treatments with statistically different length-to-width ratios compared to the water control. All statistical analyses were performed in SPSS.

Identification of tryptophanase homologs in bacterial genomes & determining indole concentration in biological samples

The presence of the tryptophanase gene (*tnaA*) in bacterial isolates cultured from the worm microbiome was determined by searching assembled and annotated genomes of bacteria isolated from *D. japonica* for *ttaA* gene annotations. The *ttaA* gene of *E. coli* strain BW25113 was also used in a tBLASTx search of these genomes.

To measure indole present in biological samples, we used the hydroxylamine-based indole assay (HIA) (Darkoh et al., 2015). Unlike the Kovács assay, this colorimetric assay specifically detects indole and does not detect other indole analogs. To determine whether bacteria isolated from the *D. japonica* microbiome were capable of producing indole, pure cultures were incubated aerobically at room temperature in tryptophan broth (TB: 10.0 g of casein enzymic hydrolysate, 1.0 g DL-tryptophan, and 5.0 g of sodium chloride in 1.0 L of water) for 2 days. Prior to inoculation, each isolate was cultured in 5 mL of TB for 2 days, then cells were pelleted by centrifugation at 10,000 g for 5 minutes, the supernatant decanted, and the cells washed twice with 5 mL of 1x PBS. After rinsing, cells were resuspended in 2.5 mL of PBS, and the OD 600 nm was measured for each sample. Using the OD measurements, samples were standardized and diluted in PBS to the isolate with the lowest OD reading. Once standardized for growth, 200 µL of the cell suspension was added to 5 mL of TB, and the culture tubes were incubated as previously described. After 2 days of growth, cultures were centrifuged as previously described to pellet cells, and the supernatant was used to quantify indole production. For each isolate, 3 replicates were used. To determine the concentration of indole of bacterial inocula in the presence of regenerating worm fragments, 700 µL of an individual inoculum was sampled, cellular debris pelleted, and the supernatant used as input for the HIA assay.

Worm regeneration screen with bacteria inoculum supplemented with tryptophan

To determine whether bacterial derived-indole can modulate regenerative outcomes in worm fragments, bacterial inocula were cultured for four bacterial strains: *Aquitalea* sp. FJL05,

Oxalobacteraceae sp. KBW02, *E. coli* BW25311, and *E. coli* JW3686-7 ($\Delta tnaA$). *E. coli* strains were obtained from the *E. coli* Genetic Stock Center at Yale University. All isolates were initially cultured in BHI and washed with 1x PBS as previously described. After the final wash, cells were resuspended in sterile worm water supplemented with or without tryptophan (4.9 mM). The OD of cell suspensions were measured as described above, and all samples were diluted to an OD of 0.3. To each inoculum, 5 trunk fragments were added and 3 replicates of 5 trunks were performed for each bacterial strain and treatment condition. After 2 days of treatment, regenerating trunk fragments were washed twice in sterile worm water and then transferred into sterile worm water for the remainder of the experiment. Over the course of the experiment, worms were examined for survival of fragments, eye spot development, and overall body shape development. Throughout the experiment, representative images were taken for each replicate at 3 and 4 days post-amputation, with all regenerating fragments imaged at 7 and 12 days post-amputation. Indole concentrations were determined at 0, 2, and 4 days post-amputation for all treatment conditions by sampling 100 μ L of the suspension solution containing regenerating worm fragments using the HIA assay (described above).

SUPPLEMENTAL REFERENCES

- Aziz, R.K., Bartels, D., Best, A.A., DeJongh, M., Disz, T., Edwards, R.A., Formsma, K., Gerdes, S., Glass, E.M., Kubal, M., Meyer, F., Olsen, G.J., Olson, R., Osterman, A.L., Overbeek, R.A., McNeil, L.K., Paarmann, D., Paczian, T., Parrello, B., Pusch, G.D., Reich, C., Stevens, R., Vassieva, O., Vonstein, V., Wilke, A., Zagnitko, O., 2008. The RAST Server: rapid annotations using subsystems technology. BMC Genomics 9, 75.
- Caporaso, J.G., Lauber, C.L., Walters, W.A., Berg-Lyons, D., Lozupone, C.A., Turnbaugh, P.J., Fierer, N., Knight, R., 2011. Global patterns of 16S rRNA diversity at a depth of millions of sequences per sample. Proceedings of the National Academy of Sciences 108, 4516–4522.
- Darkoh, C., Chappell, C., Gonzales, C., Okhuysen, P., 2015. A rapid and specific method for the detection of indole in complex biological samples. Appl. Environ. Microbiol. 81, 8093–8097.
- David, L.A., Maurice, C.F., Carmody, R.N., Gootenberg, D.B., Button, J.E., Wolfe, B.E., Ling, A.V., Devlin, A.S., Varma, Y., Fischbach, M.A., Biddinger, S.B., Dutton, R.J., Turnbaugh, P.J., 2014. Diet rapidly and reproducibly alters the human gut microbiome. Nature 505, 559–563.
- Kastman, E.K., Kamelamela, N., Norville, J.W., Cosetta, C.M., Dutton, R.J., Wolfe, B.E., 2016. Biotic interactions shape the ecological distributions of *Staphylococcus* species. MBio 7, e01157–16.
- Lane, D.J., 1991. 16S/23S rRNA sequencing. In “Nucleic acid techniques in bacterial systematics”.(Eds E Stackebrandt, M Goodfellow) pp. 115–175.
- Lee, F.J., Rusch, D.B., Stewart, F.J., Mattila, H.R., Newton, I.L.G., 2015. Saccharide breakdown and fermentation by the honey bee gut microbiome. Environ. Microbiol. 17, 796–815.
- Oviedo, N.J., Nicolas, C.L., Adams, D.S., Levin, M., 2008. Establishing and maintaining a colony of planarians. CSH Protoc. 2008, db.prot5053.
- Schloss, P.D., Westcott, S.L., Ryabin, T., Hall, J.R., Hartmann, M., Hollister, E.B., Lesniewski, R.A., Oakley, B.B., Parks, D.H., Robinson, C.J., Sahl, J.W., Stres, B., Thallinger, G.G., Van Horn, D.J., Weber, C.F., 2009. Introducing mothur: open-source, platform-independent, community-supported software for describing and comparing microbial communities. Appl. Environ. Microbiol. 75, 7537–7541.
- Turner, S., Pryer, K.M., Miao, V.P., Palmer, J.D., 1999. Investigating deep phylogenetic relationships among cyanobacteria and plastids by small subunit rRNA sequence analysis. J. Eukaryot. Microbiol. 46, 327–338.
- Wolfe, B.E., Button, J.E., Santarelli, M., Dutton, R.J., 2014. Cheese rind communities provide tractable systems for in situ and in vitro studies of microbial diversity. Cell 158, 422–433.